AMERICAN SOCIETY FOR MICROBIOLOGY | Molecular and Cellular Biology®

RESEARCH ARTICLE

Negative Feedback Loop Mechanism between EAF1/2 and DBC1 in Regulating ELL Stability and Functions

Subham Basu,[a] Arijit Nandy,[a] Mahesh K. Barad,[a] Sujay Pal,[a] Debabrata Biswas[a]

[a]Laboratory of Transcription Biology, Molecular Genetics Division, CSIR-Indian Institute of Chemical Biology, Kolkata, West Bengal, India

Subham Basu and Arijit Nandy contributed equally to this work. The order of the authors were determined based on their overall contribution in this study.

ABSTRACT Although ELL-associated factors 1 and 2 (EAF1/2) have been shown to enhance RNA polymerase II-mediated transcription *in vitro*, their functional roles *in vivo* are poorly known. In this report, we show functions of these proteins in regulating ELL stability through their competitive binding with HDAC3 at the N terminus of ELL. Reduced HDAC3 binding to ELL causes increased acetylation leading to reduced ubiquitylation-mediated degradation. Similar functional roles played by DBC1 in regulating ELL stability further prompted in-depth analyses that demonstrated presence of negative feedback loop mechanisms between DBC1 and EAF1/2 in maintaining overall ELL level. Mechanistically, increased DBC1 reduces EAF1/2 level through increased ubiquitylation involving E3 ubiquitin ligase TRIM28, whereas increased EAF1/2 reduces DBC1 level through reduced transcription. Physiologically, after a few passages, ELL levels in either DBC1 or EAF1 knockdown cells are restored through enhanced expression of EAF1 and DBC1, respectively. Interestingly, for maintenance of ELL level, mammalian cells prefer the EAF1-dependent pathway during exposure to genotoxic stress, and the DBC1-dependent pathway during exposure to growth factors. Thus, we describe coordinated functions of multiple factors, including EAF1/2, HDAC3, DBC1, and TRIM28 in regulating ELL protein level for optimal target gene expression in a context-dependent manner within mammalian cells.

KEYWORDS DBC1, EAF1, ELL, HDAC3, super elongation complex, TRIM28, transcriptional regulation, ubiquitylation

Although initiation of transcription is considered to be rate-limiting for regulation of expression of multiple sets of genes, recent studies have also shown a role for promoter proximal pausing in transcriptional regulation of genes that are expressed either during different stages of development or in response to various stress signals (1–3). Upon release from promoter proximal pausing, RNA polymerase II (Pol II, hereafter) enters the productive elongation step and comes under the regulation of various elongation factors for faithful transcription of target genes (4).

Among all the transcription elongation factors, the recently described super elongation complex (SEC) has gained significant attention predominantly because of its diverse role in transcriptional regulation as well as its involvement in various human diseases (5–9). Human SEC is a megadalton complex containing AFF1/AFF4, AF9/AF9 family-related protein ENL, either ELL or its isoforms ELL2/3, ELL-associated factors 1/2 (EAF1/2), and P-TEFb complex. Human P-TEFb complex is a heterodimer of CyclinT1/2 and CDK9 (10, 11) that phosphorylates several proteins, including DRB sensitivity inducing factor (DSIF), negative elongation factor (NELF) as well as the C-terminal domain (CTD) of Pol II during pausing at the promoter proximal region for assisting its entry into productive elongation. Our studies and others have shown a role of several initiation as well as other transcription factors in regulating SEC as well as P-TEFb

Address correspondence to Debabrata Biswas, dbiswas@iicb.res.in.

The authors declare no conflict of interest.

Received 20 April 2022
Returned for modification 5 June 2022
Accepted 8 August 2022
Published 29 August 2022

complex recruitment for transcriptional regulation at the promoter proximal region (12–17).

Among all the SEC components, ELL is the only bona fide elongation factor that directly stimulates transcription elongation by Pol II through reducing the rate of transient pausing during elongation (8, 18). Several other ELL-interacting proteins within the SEC have been shown to assist ELL function during transcriptional elongation (19, 20). Although EAF1 and EAF2 have been described as strong ELL-interacting proteins previously (21–23), their overall role in ELL-mediated transcriptional regulation is still poorly known.

An initial breakthrough in understanding a role of EAF1 and EAF2 in ELL-mediated transcription was described by Conaway's lab, showing a positive role of these two factors in ELL-assisted Pol II-mediated transcriptional elongation *in vitro* (19). Subsequently, our studies confirmed this function of EAF1 and EAF2 in overall positive regulation of ELL-assisted Pol II-mediated transcription elongation (8). Although *in vitro* studies have shown redundant functions of EAF1 and EAF2 in stimulation of ELL-mediated Pol II-dependent transcription elongation, similar functional roles of these proteins within mammalian cells are yet to be reported. Further studies showed a role of EAF1 in MED26 (a subunit of Mediator complex)-dependent recruitment of SEC at the promoter proximal region for transcriptional regulation (12). Our recent study has also shown a role of EAF1 and AF9 in TFIID-dependent recruitment of SEC at the promoter proximal region for assisting the transition of paused Pol II to productive elongation (13). However, besides these studies, the overall role of EAF1 and EAF2 in regulation of ELL function, especially in relation to its stabilization (if any), is completely unknown.

In this study, we report a novel role of human EAF1 and EAF2 in regulating ELL stability through reduced HDAC3-mediated deacetylation and subsequent ubiquitin proteasome-mediated degradation. Since our recent study also showed the similar role of human DBC1 in regulation of ELL stability (24), further in-depth study showed presence of a feedback loop mechanism between DBC1 and EAF1 in regulation of ELL stability within mammalian cells. Thus, we describe coordinated functions of multiple factors, including EAF1/2, HDAC3, DBC1, and the ubiquitin E3 ligase TRIM28 in regulation of ELL stability within mammalian cells.

RESULTS

EAF1 and EAF2 stabilize ELL within mammalian cells. While reconfirming possible interaction between ectopically expressed ELL and EAF1 within mammalian cells, we were surprised to observe a dose-dependent effect of EAF1 expression on increasing expression of ectopic ELL protein (Fig. 1A, compare lane 2 versus lanes 4–6, blots in the upper panel and quantification of ELL protein in the lower panel), even though the same amount of ELL plasmid constructs were transfected in each assay. Subsequent qRT-PCR analyses showed that while the EAF1 mRNA level is expressed in increasing amounts (with increasing transfection) (Fig. S1A, upper panel), the ELL mRNA level is very modestly increased (Fig. S1A, lower panel), thus indicating an effect of EAF1 on regulating ELL protein level. Not surprisingly, like EAF1, ectopically expressed EAF2 also shows similar effect on overall expression of ectopic ELL protein within mammalian cells (Fig. 1B, compare lane 2 versus lanes 4–6, blots in the upper panel and quantification of ELL protein in the lower panel) without increasing its mRNA level (Fig. S1B, lower panel) despite increasing expression of EAF2 mRNA (Fig. S1B, upper panel). All these results indicate potential roles of EAF1 and EAF2 in modulating the stabilization of ELL protein level within mammalian cells.

Overexpression of EAF1 also increased the expression of endogenous ELL (Fig. S1C, compare lane 1 versus lanes 2–4, blots in the upper panel and quantification of ELL protein in the lower panel). Simultaneous knockdown of both EAF1 and EAF2 reduced the expression of endogenous ELL protein when compared to control scramble knockdown (Fig. 1C), thus providing further evidence of this regulation in an endogenous context. Overall, we conclude that the human EAF1 and EAF2 may regulate ELL protein

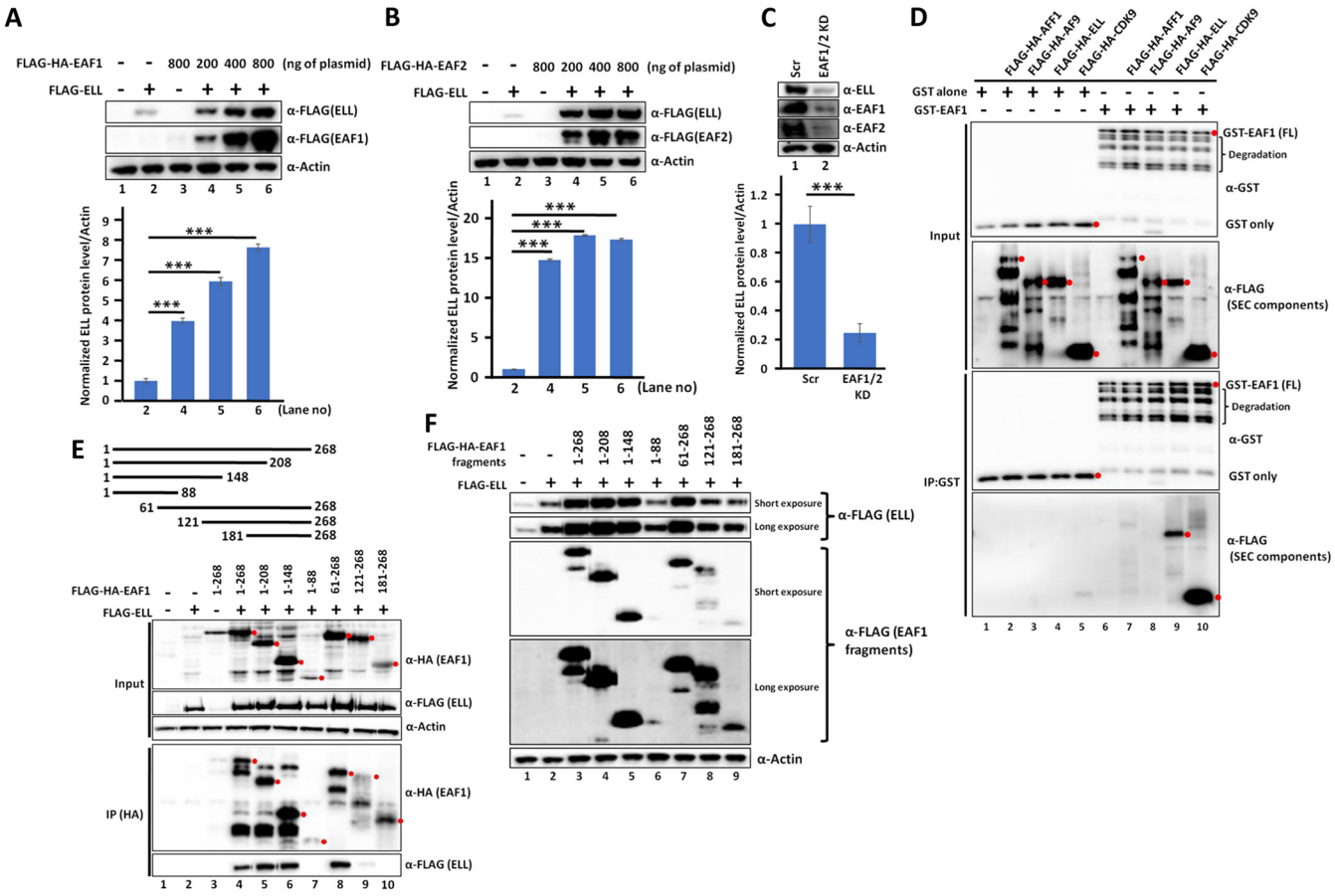

FIG 1 EAF1 and EAF2 stabilize ELL protein within mammalian cells. (A) Western blot analysis showing the effect of overexpression of EAF1 on ectopically expressed ELL within 293T cells (top panel). The lower panel shows the quantification of ELL protein levels with respect to actin. The amount of EAF1 plasmid being used in each experiment is mentioned in ng. (B) Western blot analysis showing the effect of overexpression of EAF2 on ectopically expressed ELL within 293T cells (top panel) and quantification of ELL protein levels relative to actin (bottom panel). The amount of EAF2 plasmid being used in each experiment is mentioned in ng. (C) Immunoblots showing shRNA-mediated stable knockdown of EAF1 and EAF2 in 293T cells and the effect of this depletion on endogenous ELL protein levels. The lower panel shows the quantification of ELL protein levels with respect to actin. (D) *In vitro* interaction analysis and subsequent immunoblots showing direct interaction between EAF1 and indicated SEC components. Interestingly, along with ELL, CDK9 was also seen to interact with EAF1 *in vitro*, whereas other SEC members failed to do so. The bands marked with filled red dots represent the target protein bands. Others represent either degradation or nonspecific bands. In all reaction sets, 500 ng of each protein were added as per the reaction mixture prepared. (E) Coimmunoprecipitation and Western blotting showing interaction of the indicated EAF1 domains (top panel) with ectopically expressed ELL in 293T cells. The bands marked with filled red dots represent the target protein bands. (F) Cotransfection and subsequent Western blotting showing the effect of different EAF1 domains in the stabilization of ectopically expressed ELL. The EAF1 fragments that retain ELL interaction region can stabilize ELL within 293T cells. In all our statistical analyses, the data represents a minimum of $n = 2$ biological replicates and 3 technical replicates of each biological replicate. Statistical analyses were performed using one-tailed Student's t test wherein * denotes $P \leq 0.05$, *** denotes $P \leq 0.001$, and ns denotes not significant.

level within mammalian cells by potentially affecting its stability rather than its mRNA expression.

Direct interaction of ELL with EAF1 and EAF2 is required for its stabilization. Next, we addressed whether the overall effect on ELL stabilization by EAF1/2 is specific to only this SEC component. As shown in Fig. S1D, cotransfection of EAF1 only increased expression of ELL protein (compare lane 11 versus lane 12) and not of other SEC components. In fact, overexpression of EAF1 reduced the expression of ectopic AFF1, AFF4, and AF9 components (Fig. S1D, compare lanes 3–8 in presence or absence of EAF1). Interestingly, in our analysis, we have reproducibly observed a very modest effect of EAF1 on increasing expression of CDK9 (compare lane 9 versus lane 10).

Further, we addressed whether the specificity of EAF1 stabilization is a result of its direct interaction with specific SEC components. We purified AFF1, AF9, ELL, and CDK9 (of P-TEFb complex) components of SEC through their overexpression in mammalian cells (Fig. S1E, lanes 3–6) (25) and GST-EAF1 through its expression in bacterial systems

(Fig. S1E, lane 2). *In vitro* direct interaction analyses clearly showed the presence of direct interaction between EAF1 and ELL as well as CDK9 (Fig. 1D, lane 9 and 10) but not other SEC components. Therefore, earlier reported EAF1 interaction with different SEC components by other studies (26, 27) could also be a result of direct EAF1 interaction with ELL and CDK9 that, in turn, directly interact with other SEC components. These analyses clearly indicate an essential role of direct interaction in EAF1-mediated ELL stabilization within mammalian cells.

For deeper understanding of the overall mechanisms in these regulations, we generated several EAF1 constructs with 60 amino acid deletions from both N- and C-terminal ends in a mammalian expression vector (Fig. 1E, upper panel). Subsequent coimmunoprecipitation (co-IP) analyses showed that deletion of the region between 89 and 148 amino acids from the C-terminal end (Fig. 1E, lane 7, IP panel) and between 61 and 120 amino acids from the N-terminal end completely abolished EAF1 interaction with ELL (Fig. 1E, lane 8 versus lane 9). Therefore, we conclude that the region between 89 and 120 amino acids within EAF1 is absolutely critical for its interaction with ELL. For providing direct evidence of this domain-dependent EAF1-ELL interaction, we purified GST-tagged full-length as well as the above-mentioned domains of EAF1 and ELL (as His-GFP epitope-tagged) through their expression in bacterial systems (Fig. S1F and S1G). Subsequent *in vitro* direct interaction assays clearly showed, whereas fragments containing 89–148 region retained ELL interaction (Fig. S1H, lanes 5–7 and 9), the other fragments lacking these regions failed to do so when compared to full-length EAF1 (lanes 8 and 10–11). Thus, we conclude that the region between amino acids 89 and 120 of EAF1 is absolutely important for its direct interaction with ELL.

Our next cotransfection analyses using these EAF1 fragments along with ELL showed that although full-length and other deletion fragments of EAF1 containing the region 89 to 120, stabilized ELL (Fig. 1F, lanes 3–5 and 7), deletion fragments lacking the 89 to120 region of EAF1 failed to do so (Fig. 1F, compare lanes 3–5 and 7 with lanes 6, and 8–9) when all these EAF1 fragments are expressed at similar levels (Fig. 1F, FLAG-HA-EAF1 fragments). Thus, based on our stabilization and interaction analyses, we conclude that an EAF1 interaction with ELL is required for stabilization of ELL and the region between amino acids 89 and 120 shows maximum effect on stabilization of ELL within mammalian cells.

EAF1 and EAF2 protect ELL against ubiquitin-mediated degradation within mammalian cells. Based on our recent report that ELL protein is subjected to ubiquitin proteasome-mediated degradation within mammalian cells (24), we checked whether EAF1 and EAF2 could protect ELL from this degradation. As shown in Fig. 2A, and consistent with our earlier report, in the presence of exogenously overexpressed ubiquitin, ELL protein is degraded within mammalian cells (Fig. 2A, compare lane 2 versus lane 3). Interestingly, concomitant overexpression of either EAF1 or EAF2 fully rescued this degradation of ELL (Fig. 2A, compare lane 3 versus lanes 4–6 and 7–9). Consistent with its sensitivity, in the presence of overexpressed ubiquitin, ubiquitination level of ELL is also increased (Fig. 2B, lane 2). Further, consistent with the role of EAF1 and EAF2 in rescuing ubiquitin-mediated ELL degradation, we have also observed marked reduction of ELL ubiquitination level when EAF1/2 proteins are coexpressed (Fig. 2B, compare lane 2 versus lanes 3–5 and 6–8). Overexpression of ubiquitin promoted ELL degradation kinetics in our cycloheximide (CHX) chase assay (Fig. 2C, compare lanes 1–3 versus 4–6), and overexpression of either EAF1 or EAF2 markedly reduced this degradation rate (Fig. 2C, compare lanes 4–6 versus 7–12). Thus, we conclude that human EAF1 and EAF2 reduce ubiquitin-mediated ELL degradation kinetics within mammalian cells.

In our recently published study, we have also reported that human ELL protein is specifically subjected to HDAC3-mediated deacetylation of key lysine residues at its N-terminal end that are also subjected to ubiquitination by Siah1 E3 ubiquitin ligase, thus promoting its degradation (24). Interestingly, as shown in Fig. 2D, overexpression of either EAF1 or EAF2 rescued HDAC3-mediated ELL degradation as well (Fig. 2D, compare lane 4 versus lanes 5–7 and 8–10). Further, overexpression of EAF1 or EAF2 also reduced HDAC3-mediated enhanced ELL ubiquitination and degradation (Fig. 2E,

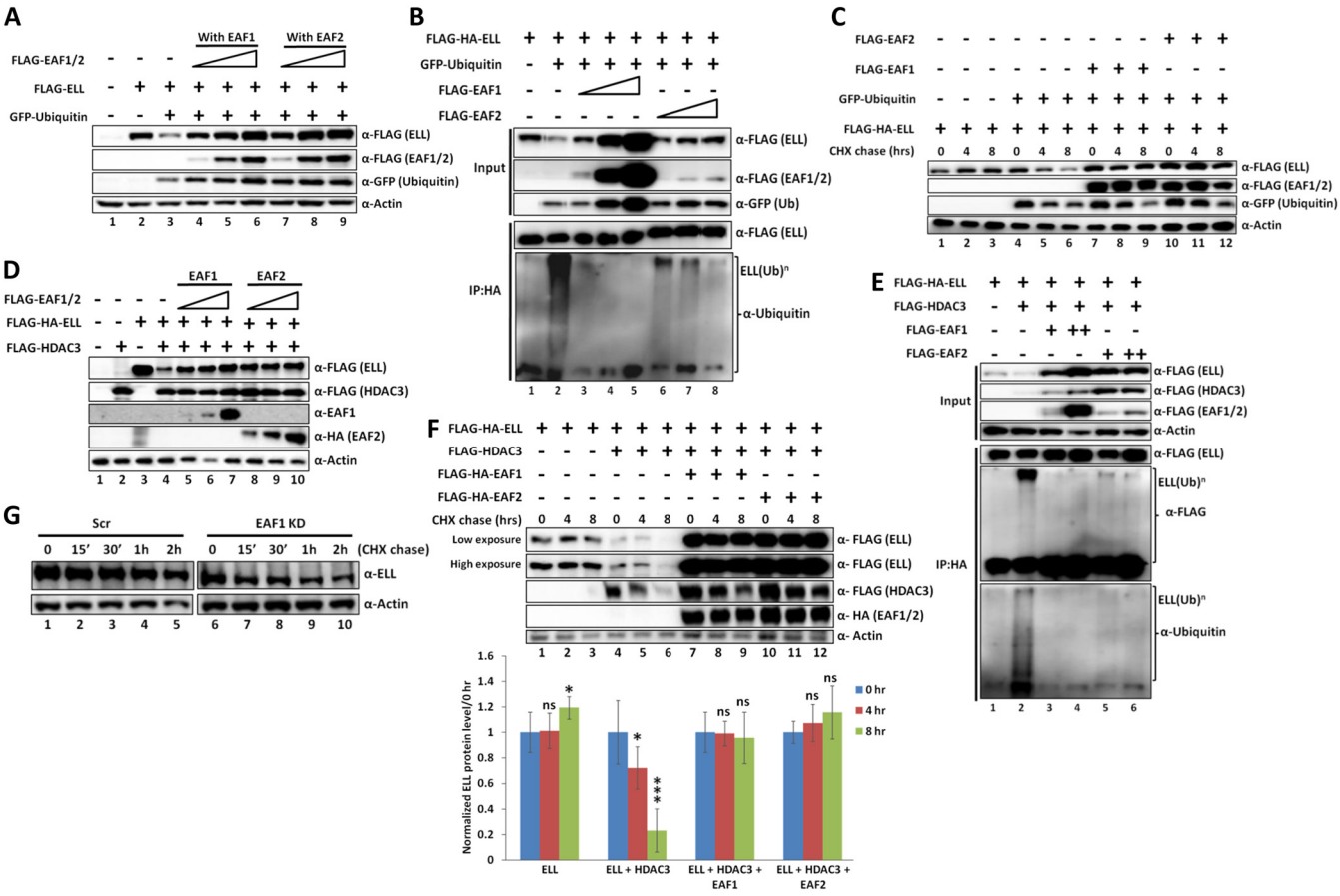

FIG 2 EAF1 and EAF2 stabilize against ubiquitin and HDAC3-mediated ELL degradation within mammalian cells. (A) Western blotting showing rescue of ubiquitin-mediated ELL degradation by overexpression of EAF1 and EAF2 within 293T cells. (B) Immunoblotting analysis showing decreased ELL polyubiquitination in the presence of ubiquitin upon concomitant overexpression of EAF1 and EAF2. (C) CHX chase assay showing increased ELL degradation kinetics in the presence of ubiquitin which is reduced upon overexpression of EAF1 and EAF2 within 293T cells. (D) Western blotting showing rescue of HDAC3-mediated ELL degradation by overexpression of EAF1 and EAF2 within 293T cells. (E) Immunoblots showing decreased ELL polyubiquitination in the presence of HDAC3 upon concomitant overexpression of EAF1 and EAF2 within 293T cells. (F) CHX chase assay showing enhanced ELL degradation kinetics in the presence of HDAC3 that can be rescued through concomitant overexpression of EAF1 and EAF2 within 293T cells (top panel). The lower panel shows the quantification of ELL protein levels with respect to actin and further renormalized to the 0′ time point. The significance value is shown with respect to the 0 h time point of each combination of experiment. The data represents a minimum of $n = 2$ biological replicates and 3 technical replicates of each biological replicate. Statistical analyses were performed using one-tailed Student's t test wherein * denotes $P \leq 0.05$, *** denotes $P \leq 0.001$, and ns denotes not significant. (G) CHX chase assay showing increased degradation kinetics of endogenous ELL upon knockdown of EAF1 within 293T cells.

compare lane 2 versus lanes 3–4 and 5–6). Consistent with this observation, we have also observed significant reduction in HDAC3-mediated ELL degradation kinetics in the presence of overexpressed EAF1 or EAF2 (Fig. 2F, compare lanes 4–6 versus 7–9 and 10–12, top panel for blots and bottom panel for quantification).

Next, for providing evidence of this mechanism of ELL stability within mammalian cells, we knocked down EAF1 that resulted in reduced expression of ELL under normal growth condition (Fig. 2G, compare lane 1 versus lane 6). Consistent with our earlier report (24), within the time period of our CHX chase assay, ELL level remains somewhat stable. However, knockdown of EAF1 markedly enhanced ELL degradation kinetics (Fig. 2G, compare lanes 2–5 versus 7–10) that somewhat mirrored the effect of overexpression of HDAC3 (Fig. 2F, lanes 4–6). These results thus predict that both EAF1 and EAF2 act in opposition to HDAC3 that promotes ubiquitination-mediated ELL degradation within mammalian cells.

N-terminal region of ELL is critical for its interaction with EAF1/2 and HDAC3. Our results in Fig. 2 indicate that the HDAC3 and EAF1/2 act in opposition toward regulating ELL stability. For deeper understanding of the mechanism of these regulations, we initially sought to address whether HDAC3 and EAF1 or EAF2 would compete with

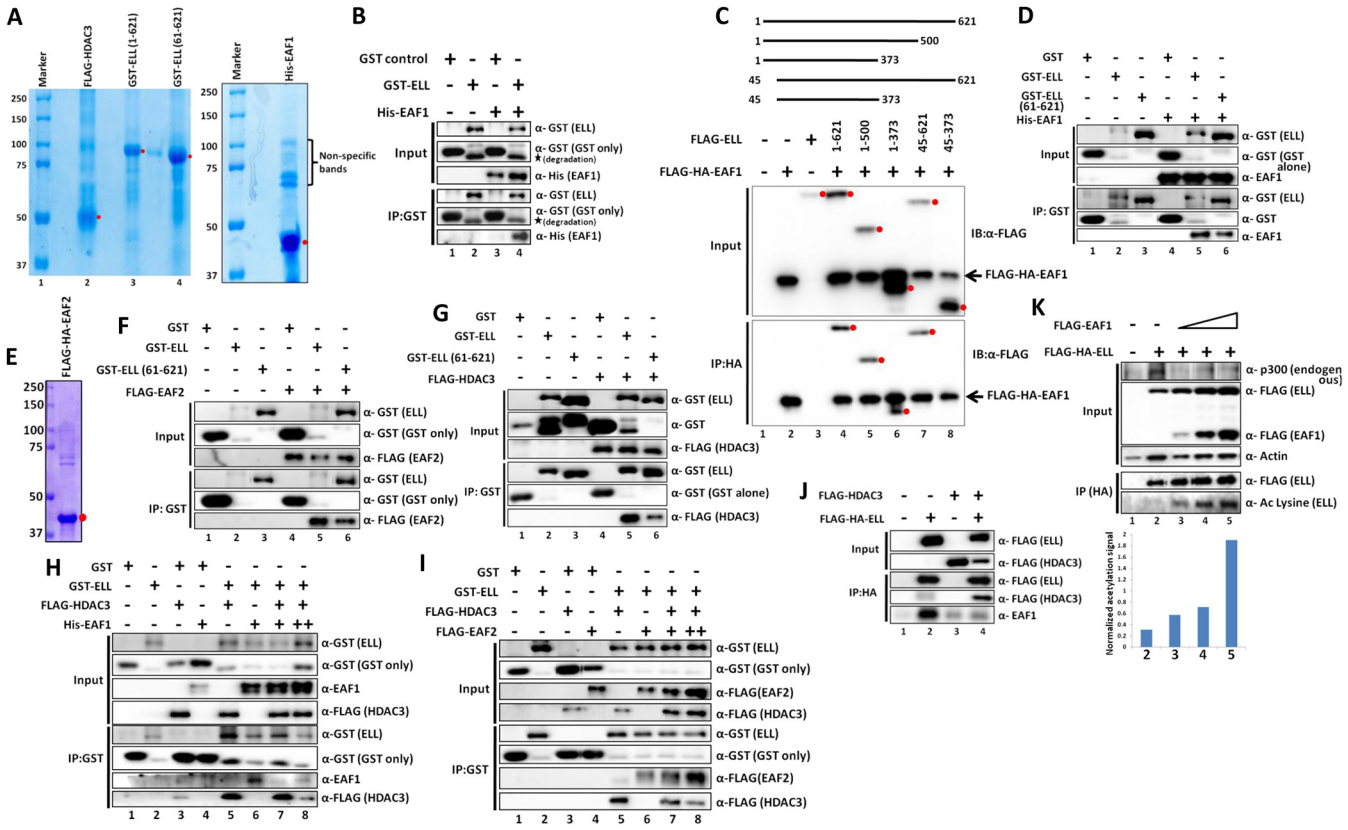

FIG 3 EAF1 and EAF2 compete with HDAC3 toward binding to the N terminus of ELL and protect its acetylation. (A) Coomassie staining of purified recombinant FLAG-HDAC3 (through expression in 293T cells), GST-ELL (full-length, 1–621), and GST-ELL (61–621) (through expression in bacterial expression system). The bands marked with filled red dots represent the target protein bands. (B) *In vitro* direct interaction analysis with purified proteins to show interaction of EAF1 with GST-ELL but not GST alone. In this experimental setup, 500 ng of GST-ELL and 1 μg of GST alone were used immobilized on agarose beads in each reaction, and 500 ng of EAF1 was added to respective reaction mixtures as the prey protein. (C) Coimmunoprecipitation and subsequent immunoblotting analysis showing the interaction of EAF1 with indicated different domains of ELL within 293T cells. Ectopically expressed FLAG-HA-EAF1 was immunoprecipitated using α-HA agarose beads and associated ELL fragments were identified through immunoblots using α-FLAG antibody. The bands marked with filled red dots represent the target ELL proteins. (D) *In vitro* direct interaction assay with purified proteins showing the critical role of the N terminus (60 amino acids) of ELL in its interaction with EAF1. GST alone was used as a control in this experiment. 500 ng of GST-ELL and 1 μg of GST alone were used immobilized on agarose beads in each reaction. 500 ng of EAF1 was added to respective reaction mixtures as the prey protein. (E) Coomassie staining of purified recombinant FLAG-HA-EAF2 (through expression in 293T cells). (F) *In vitro* direct interaction assay with purified proteins showing the critical role of the N terminus (60 amino acids) of ELL in its interaction with EAF2. GST alone was used as a control in this experiment. For this, 500 ng of GST-ELL and 1 μg of GST alone were used immobilized on agarose beads in each reaction. While 500 ng of EAF2 was added to respective reaction mixtures as the prey protein. (G) *In vitro* direct interaction assay with purified proteins showing the critical role of the N terminus (60 amino acids) of ELL in its interaction with HDAC3. GST alone was used as a control in this experiment. In this experimental setup, 500 ng of GST-ELL and 1 μg of GST alone were used as immobilized on agarose beads for each reaction. 500 ng of HDAC3 was added to respective reaction mixtures as the prey protein. (H) *In vitro* competitive binding assay using purified GST-ELL, EAF1, and HDAC3 showing decreased association of HDAC3 with ELL upon increased binding with EAF1. For this competitive binding assay, 500 ng of GST-ELL and 1 μg of GST alone were used immobilized on agarose beads for each reaction. While 500 ng of HDAC3 was added in each reaction mix, for testing if EAF1 could inhibit ELL-HDAC3 interaction, 500 ng and 1 μg of EAF1 were used. (I) *In vitro* competitive binding assay using purified GST-ELL, EAF2, and HDAC3 showing decreased association of HDAC3 with ELL upon increased binding with EAF2. In this assay, 500 ng of GST-ELL and 1 μg of GST alone were used as immobilized on agarose beads for each reaction. While 500 ng of HDAC3 was added in each reaction mix, and for testing the effect of EAF2 on ELL-HDAC3 association, 500 ng and 1 μg of EAF2 were used in the respective reactions. (J) Immunoprecipitation and Western blotting showing decreased ELL-EAF1 association in the presence of overexpressed HDAC3 within 293T cells. (K) The presence of EAF1 results in an increase in ELL acetylation level within 293T cells as observed by immunoprecipitation and Western blotting (top panel). The bottom panel depicts a quantification of the ELL acetylation signal in the presence of EAF1.

each other for their binding to ELL and thus regulate opposing functions. For addressing direct evidence of this mechanism, we purified HDAC3 as well as ELL and EAF1 through their expression in mammalian and bacterial cells (Fig. 3A). Subsequent *in vitro* analysis showed presence of direct interaction between ELL and EAF1 (Fig. 3B, lane 4). This interaction is specific to ELL only since in the same experiment, control GST alone failed to show any interaction (Fig. 3B, lane 3). Consistent with earlier reports (19, 21), coimmunoprecipitation analyses further showed critical role of N-terminal 44 amino acids of ELL for its interaction with EAF1. N-terminal 44 amino acid-deleted ELL (45–621) showed marked reduction in its interaction with EAF1, when compared with full-

length (1–621) (Fig. 3C, compare lane 4 versus lane 7). Further, an N-terminal fragment (45–373) deleted of these 44 amino acids, completely lost its interaction with EAF1 (Fig. 3C, compare lane 6 with lane 8) within mammalian cells. Consistent with this, *in vitro* analysis using the N-terminal 60 amino acid-deleted ELL fragment showed marked reduction in ELL interaction with EAF1 (Fig. 3D, compare lane 5 with lane 6 and Fig. S2A for quantification). Similar results are also observed by *in vitro* interaction assays with purified EAF2 (Fig. 3E), wherein, an N-terminal deletion of 60 amino acids markedly reduced ELL interaction with EAF2 as well (Fig. 3F, compare lane 5 versus lane 6 and Fig. S2B for quantification). Further, cotransfection of ELL fragments with full-length EAF1 showed a critical role of the N-terminal 44 amino acids in its overall stabilization since ELL constructs containing this deletion failed to show any stabilization by EAF1 (Fig. S2C compare lanes 2–7 with lanes 8–13).

Next, using purified proteins, we also observed direct interactions between ELL and HDAC3 (Fig. 3G, lane 5) as reported previously (24). Interestingly, deletion of the same N-terminal 60 amino acids significantly reduced ELL interaction with HDAC3 (Fig. 3G, compare lane 5 versus lane 6 and S2D for quantification). These observations clearly suggested the presence of competition between EAF1/2 and HDAC3 for their interaction with ELL owing to their same binding sites at the N terminus.

Both EAF1 and EAF2 compete with HDAC3 for their binding to ELL. Based on our above-mentioned results, we performed *in vitro* studies for addressing competition between EAF1 and EAF2 with HDAC3 for their binding to ELL. As shown in Fig. 3H, increasing concentration of purified EAF1 in the reaction and their binding to ELL markedly reduced ELL interaction with HDAC3 (compare lane 5 with lanes 7–8). Similar results were also obtained using purified EAF2, wherein, increased binding of EAF2 also reduced concomitant binding of HDAC3 to ELL (Fig. 3I, compare lane 5 with lanes 7–8). Consistent with *in vitro* studies, cotransfection of HDAC3 along with ELL showed reduced association of ELL with EAF1 upon its binding with HDAC3 within mammalian cells (Fig. 3J, compare lane 2 with lane 4). This result further confirms the presence of competitive binding between these factors within mammalian cells as well. Further, consistent with mechanisms of competitive binding, both EAF1 and HDAC3 interact with each other within mammalian cells as has been observed by cotransfection analysis in Fig. S2E.

Increased binding of EAF1 increases ELL acetylation level. Our earlier study has shown that p300-mediated ELL acetylation at K5 and K29 residues protects it from ubiquitination-mediated degradation (24). Since, EAF1 and EAF2 also increase ELL stability within mammalian cells through competitive binding with HDAC3 at its N terminus, thus resulting in decreased ubiquitination, we wondered whether increased EAF1 and EAF2 interaction would also increase ELL acetylation level through reduced HDAC3 binding. Towards addressing that, we cotransfected 293T cells with plasmids expressing ELL and increasing amount of EAF1. As shown in Fig. 3K, ELL shows a very low level of acetylation under normal conditions as measured by immunoblot analysis of immunoprecipitated samples using pan-acetyl lysine-specific antibody. However, overexpression of EAF1 significantly increased ELL acetylation level (Fig. 3K, compare lane 2 with lanes 3–5). This increased acetylation is not an indirect effect of increased endogenous p300 expression, since we have not observed any increase in p300 expression upon EAF1 overexpression within 293T cells (Fig. 3K, upper input panel). Thus, we conclude that the competitive binding between EAF1 and HDAC3 increases the EAF1-dependent ELL acetylation level. Since acetylation and ubiquitination sites within ELL are same, enhanced acetylation increases ELL stability.

EAF1 and EAF2-mediated ELL stabilization regulates expression of diverse sets of genes. For understanding the functional implications of EAF1/2-mediated ELL stabilization, we generated EAF1/2 double knockdown cells that also showed simultaneous reduced expression of ELL protein level (Fig. 4A) without showing any effect on its mRNA (Fig. 4B). An earlier report has shown global downregulation of expression of a diverse set of genes upon ELL knockdown within 293T cells (28). Interestingly, in our analyses, simultaneous knockdown of EAF1 and EAF2 affected mRNA expression of

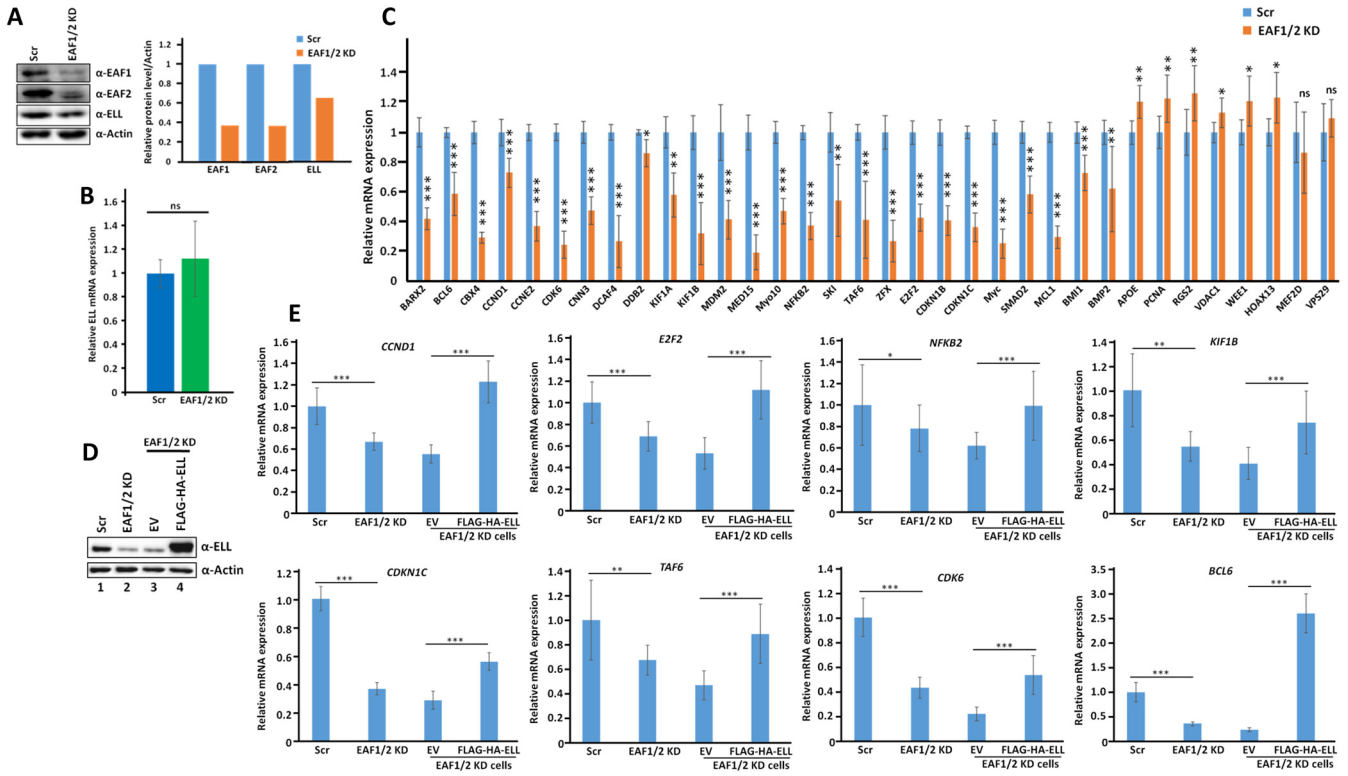

FIG 4 EAF1- and EAF2-mediated ELL stabilization is required for optimal expression of ELL-target genes. (A) Western blots showing the effect of EAF1/2 double knockdown on expression of ELL protein (left) and the quantification of protein levels compared to control scramble cells (right). (B) qRT-PCR analysis showing relative ELL mRNA levels (compared to 18s rRNA control) in scramble and EAF1/EAF2 knockdown cells. For graphical presentation, ELL mRNA levels normalized to 18s rRNA were further normalized to the value obtained in control scramble cells. (C) qRT-PCR analysis showing the effect of EAF1/2 knockdown on basal level mRNA expression of ELL target genes (compared to 18s rRNA control) in scramble and EAF1/2 knockdown cells. For graphical presentation, ELL mRNA levels normalized to 18s rRNA were further normalized to the value obtained in control scramble cells. (D) Western blot analysis showing restoration of ELL expression by its overexpression in EAF1/2 double knockdown cells. Parallel analysis with empty vector (EV) failed to restore ELL expression in these assays. Actin was used as a loading control. (E) qRT-PCR analysis showing the effect of restoration of ELL expression in EAF1/2 double knockdown cells (Fig. 6D) on expression of some of the ELL target genes as shown in Fig. 6C. As can be seen, restoration of ELL expression restored expression of target genes that were tested in our assay. Parallel transfection with control (EV) failed to do so. In these experiments, 18s rRNA was used as an internal control. For graphical presentation, ELL mRNA levels normalized to 18s rRNA were further normalized to the value obtained in control scramble cells. In these experiments qRT-PCR data represents as mean +/− SD. Student's *t* test was used to calculate the statistical significance of the data in this figure. *, $P \leq 0.05$; **, $P \leq 0.01$; ***, $P \leq 0.001$. At least $n = 2$ biological replicates were performed for each experiment.

majority of tested genes as measured by qRT-PCR analysis (Fig. 4C). This effect is specific since, in the same analysis, we have failed to observe any effect on some of the nontarget genes. Interestingly, significant numbers of these genes, including *BCL6*, *CCND1*, *CCNE2*, *CDK6*, *MYC*, and *CDKN1C*, are involved in regulation of cell proliferation. Besides, other target genes such as *CDK6*, *KIF1A*, and *KIF1B* are involved in regulation of various stages of cell division. Based on these understandings, we checked the proliferation and colony formation ability of the EAF1/2 double knockdown cells. As shown in Fig. S3A, simultaneous knockdown of both EAF1 and EAF2 significantly affected proliferation of 293T cells. Consistent with reduced proliferation potential, these knockdown cells also showed reduced colony forming ability (Fig. S3B). Thus, based on all these results, we conclude that EAF1/2-mediated ELL stabilization within mammalian cells is required for expression of diverse sets of target genes, including ones that are important for cell proliferation as well as colony formation.

Next, we addressed whether the overall effect of EAF1 and EAF2 on ELL stability is cell-type specific. Towards addressing that, we performed simultaneous knockdown of both EAF1 and EAF2 in colorectal carcinoma HCT116 cells (Fig. S3C). Knockdown of both EAF1 and EAF2 also reduced ELL protein level comparable to that of 293T cells (Fig. S3C-D). Further, a significant number of genes that showed reduced expression upon EAF1/2 knockdown in 293T cells, also showed impaired expression in HCT116 cells (Fig. S3E). Also, consistent with a role of these genes in regulating cell

proliferation, we have also observed reduced proliferation and colony forming ability of HCT116 cells (Fig. S3F and S3G) upon EAF1/2 knockdown. Thus, we conclude that the effect of EAF1 and EAF2 on regulating ELL stability and thus regulation of expression of ELL-target genes and downstream effect on cell proliferation and colony formation is not cell type-specific.

Critical requirement of ELL in EAF1/2 knockdown cells for target gene expression. Since simultaneous knockdown of EAF1/2 causes a reduced ELL level that results in impaired expression of target genes, we wondered whether ELL is the critical component in EAF1/2 knockdown cells for transcriptional downregulation of these genes. Towards addressing that, we restored ELL expression in EAF1/2 knockdown cells through its overexpression (Fig. 4D, lane 4) and tested the downstream effect on target gene expression. A parallel transfection with vector control showed no effect on reduced ELL level (Fig. 4D, lane 3). As shown in Fig. 4E and Fig. S3H, restoration of ELL expression also restored mRNA expression of all the genes that we have tested. Interestingly, restored target gene expression is more than the control scramble cells in some of the target genes and is consistent with increased level of ELL expression. A parallel vector control showed no effect on overall target gene expression. These results clearly indicate that reduced ELL level is key for overall reduced expression of ELL-target genes upon EAF1/2 knockdown.

Overall results thus clearly show that human EAF1 and EAF2 competes with HDAC3 for their binding to ELL, thus increasing its acetylation and decreasing ubiquitination level. A knockdown of EAF1/2 results in reduced level of ELL that further causes reduced expression of diverse ELL target genes. A model for this mechanism of action for transcriptional regulation is presented in Fig. S3I.

DBC1 and EAF1 negatively regulate expression of each other. We have recently reported a role of human DBC1 in regulation of ELL stability (24). Our study showed that DBC1 competes with HDAC3 for its binding at the N terminus of ELL. Since HDAC3-mediated deacetylation generates lysine residues that are subsequently being targeted by ubiquitin proteasome-mediated degradation, a competition between DBC1 and HDAC3 thus causes DBC1-mediated ELL stability. Thus, we were further interested in addressing the cross talk between DBC1 and EAF1/2 in relation to regulation of overall ELL stability. Our initial analysis with ectopically expressed EAF1 (as representative of EAF1/2 proteins) and DBC1 showed that both these proteins negatively regulate expression of each other in a dose-dependent manner (Fig. 5A, compare lane 1 with lanes 3–4, and lane 5 with lanes 6–8). A similar phenomenon is also observed for endogenous EAF1 and DBC1 proteins when one of the target proteins was ectopically overexpressed (Fig. 5B and C, respectively). Interestingly, subsequent RNA analysis showed that while the overexpression of DBC1 failed to show any effect on EAF1 mRNA expression (Fig. 5B, lower panels), the EAF1 overexpression reduced the mRNA expression of endogenous DBC1 in a dose-dependent manner (Fig. 5C, middle panel). Thus, we conclude that both the DBC1 and EAF1 negatively regulate expression of each other by two different mechanisms. While DBC1 potentially regulates the EAF1 expression at the protein level, EAF1 regulates DBC1 expression through its effect on transcription of mRNA.

DBC1 increases ubiquitination of EAF1 protein within mammalian cells. For further mechanistic understanding of these regulations, we initially addressed DBC1-mediated regulation of EAF1 protein level. Our initial analyses showed that usage of ubiquitin proteasome inhibitor (MG132) efficiently rescued DBC1-mediated degradation of endogenous EAF1 (Fig. 5D, compare lane 2 with lanes 3–5), thus suggesting a role of ubiquitin proteasome-mediated regulation of EAF1 protein level within mammalian cells. Subsequent analyses showed that human EAF1 can efficiently be degraded by overexpression of ubiquitin within mammalian cells (Fig. 5E) and this can be rescued by addition of ubiquitin proteasome inhibitor MG132 (Fig. 5F, compare lane 3 versus lanes 4–6, top panel for blots and lower panel for quantification). Overexpression of ubiquitin increased EAF1 ubiquitination and thus caused its degradation (Fig. 5G, lane 3), that could also be rescued by adding MG132 (Fig. 5G,

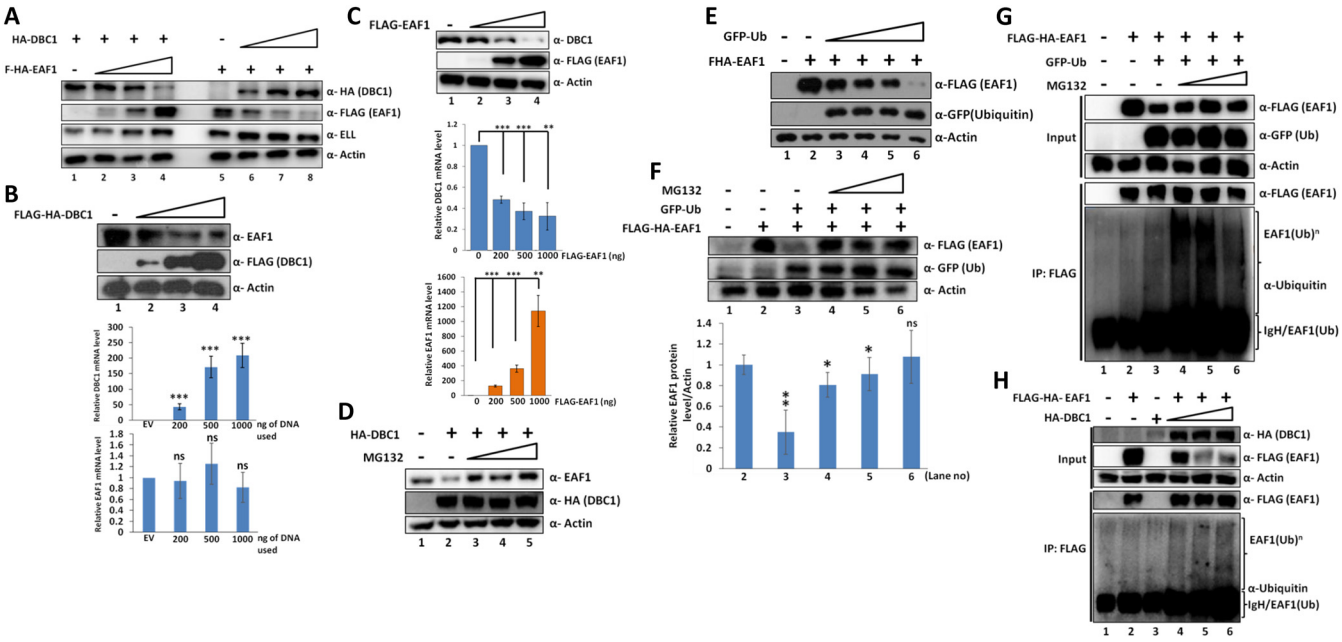

FIG 5 DBC1 and EAF1 negatively regulate expression of each other via a negative feedback loop. (A) Cotransfection and immunoblotting analyses showing the effect of ectopic overexpression of EAF1 on ectopically expressed DBC1 (lanes 1–4) and *vice versa* (lanes 5–8) in 293T cells. Overexpression of EAF1 was found to reduce DBC1 levels and *vice versa* with DBC1 overexpression having a similar effect on EAF1 as well. (B) Western blot analysis showing the effect of DBC1 overexpression on endogenous EAF1 levels in 293T cells (top panel). The bottom panel shows that EAF1 mRNA levels remain unchanged, indicating that the effect of DBC1 on EAF1 is at the protein level. (C) Western blot analysis showing the effect of EAF1 overexpression on endogenous DBC1 levels in 293T cells (top panel). The bottom panel shows that DBC1 mRNA levels decreased linearly with increasing EAF1, indicating that EAF1 may regulate DBC1 at the mRNA level. (D) Immunoblot analysis showing the rescue of DBC1-mediated EAF1 destabilization upon addition of MG132. (E) Immunoblots showing the degradation of EAF1 in the presence of increasing concentrations of ubiquitin, indicating that EAF1 is targeted for ubiquitination for its degradation. (F) Western blots showing rescue of ubiquitin-mediated EAF1 degradation by addition of MG132 (top panel). The lower panel shows the quantification of EAF1 protein levels with respect to actin. The significance value is shown with respect to lane 2 (EAF1 alone). The data represents a minimum of $n = 2$ biological replicates and 3 technical replicates of each biological replicate. Statistical analyses were performed using one-tailed Student's t test wherein * denotes $P \leq 0.05$, ** denotes $P \leq 0.01$, and ns denotes not significant. (G) Western blots showing the EAF1 ubiquitination by ectopically expressed GFP-ubiquitin. The IP panel shows polyubiquitinated species of EAF1, confirming that EAF1 does indeed undergo degradation by the ubiquitin proteasome pathway. The ubiquitin antibody used in our immunoblotting assay also nonspecifically detects the Ig heavy chain (IgH). (H) Western blots showing a similar effect of DBC1 on ectopic EAF1 as seen for ubiquitin in Fig. 7G. The IP panel shows formation of polyubiquitinated EAF1 species, indicating that DBC1 causes EAF1 polyubiquitination. The ubiquitin antibody used in our immunoblotting assay also nonspecifically detects the IgH.

compare lane 3 versus lanes 4–6). Addition of MG132 further increased EAF1 ubiquitination level. Thus, we conclude that human EAF1 protein is subjected to ubiquitin proteasome-mediated degradation within mammalian cells.

Next, we addressed, whether DBC1 would enhance EAF1 ubiquitination and thus promote its degradation. For immunoprecipitation, we used a suboptimal level of DBC1 plasmid such that coexpressed EAF1 does not get fully degraded. As shown in Fig. 5H, in the absence of DBC1 coexpression, ectopically expressed EAF1 showed modest ubiquitination that was markedly enhanced upon coexpression of DBC1 (compare lane 2 versus lanes 4–6). Thus, DBC1 could potentially regulate the expression of EAF1 through ubiquitination-mediated degradation.

DBC1 and EAF1 interact with TRIM28 ubiquitin E3 ligase. Next, we were interested in identifying mechanisms of DBC1-mediated EAF1 degradation. We were intrigued by the association of DBC1 with TRIM28 ubiquitin E3 ligase by mass spectrometry analysis of proteins associated with ectopically expressed DBC1 (24) (Fig. S4A). Subsequent immunoprecipitation analysis further confirmed DBC1 interaction with TRIM28 and EAF1 along with its known interactor ELL (Fig. S4B). Interestingly, immunoprecipitation of ectopically expressed EAF1 also showed its interaction with TRIM28 (Fig. S4C), whereas a reciprocal immunoprecipitation of ectopically expressed TRIM28 confirmed its interaction with both DBC1 and EAF1 within mammalian cells (Fig. S4D and S4E). Further, we also observed EAF1 and TRIM28 interaction when they are coexpressed within mammalian cells (Fig. S4F).

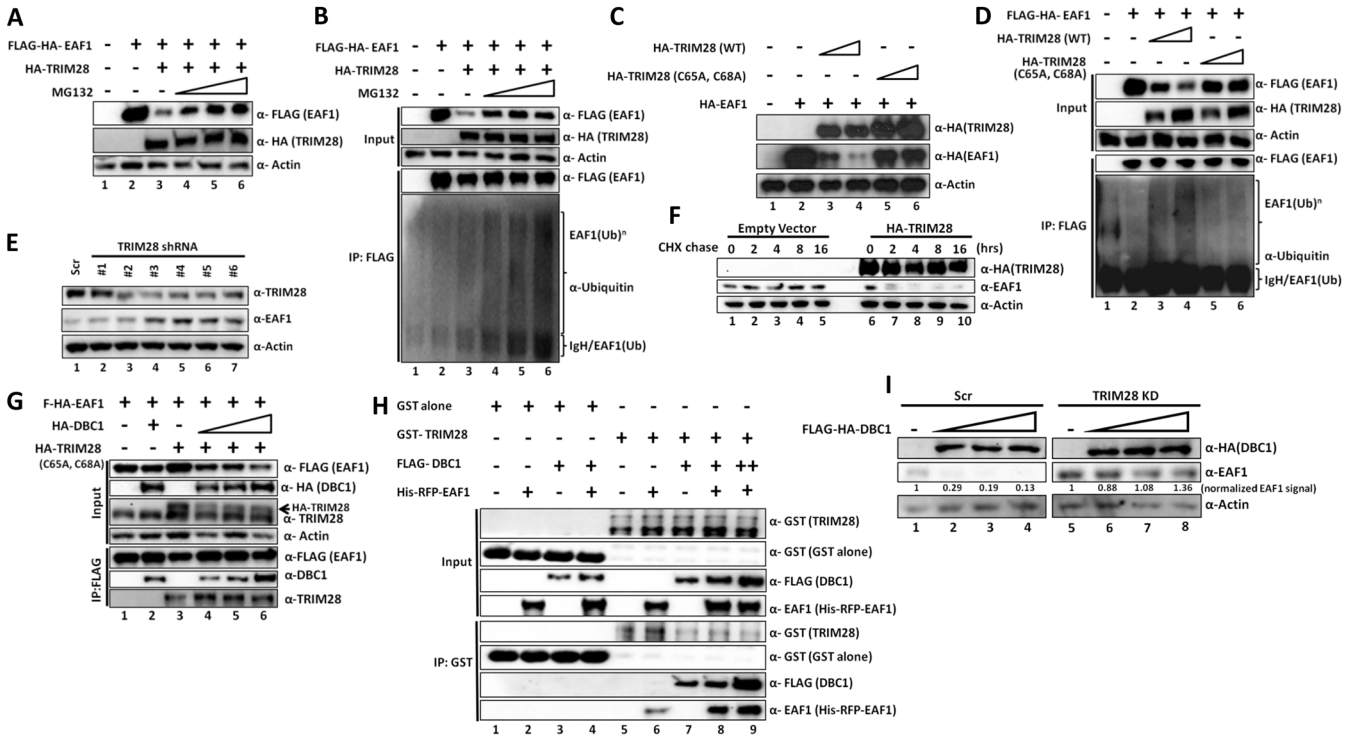

FIG 6 TRIM28 acts as the ubiquitin E3 ligase for EAF1 and DBC1 promotes EAF1 interaction with TRIM28. (A) Immunoblot analysis showing the TRIM28-mediated EAF1 degradation that can be rescued upon addition of MG132. (B) Western blot analysis showing the rescue of TRIM28-mediated EAF1 degradation upon addition of MG132 along with a subsequent significant increase in polyubiquitinated EAF1 species within 293T cells. The ubiquitin antibody used in our immunoblotting assay also nonspecifically detects the IgH. (C) Western blot analysis showing that the wild type TRIM28 can degrade ectopically expressed EAF1 but its ubiquitin E3 ligase activity deficient (C65A, C68A) mutant fails to do so. (D) Cotransfection, immunoprecipitation and subsequent Western blotting analyses showing that though the wild type TRIM28 can cause EAF1 polyubiquitination, its E3 ligase activity deficient (C65A, C68A) mutant fails to do so. The ubiquitin antibody used in our immunoblotting assay also nonspecifically detects the IgH. (E) Immunoblots indicating the levels of endogenous EAF1 in several TRIM28 stable knockdown cell lines compared to control scramble cells. Endogenous EAF1 levels were found to be increased upon knockdown of TRIM28. (F) CHX chase assay showing enhanced EAF1 degradation kinetics in the presence of overexpressed TRIM28 within 293T cells. (G) Immunoprecipitation and subsequent immunoblotting analyses showing enhanced interaction of TRIM28 with EAF1 upon its binding with DBC1 within 293T cells. Since TRIM28 causes degradation of EAF1, for the purpose of this experiment, TRIM28 catalytic dead mutant (C65A, C68A) was used. (H) *In vitro* direct interaction analysis with purified proteins showing that the presence of DBC1 greatly enhances the interaction between TRIM28 and EAF1. For this, 500 ng of GST-TRIM28 and 1 μg of GST alone were used as immobilized on agarose beads for each reaction. Similarly, 500 ng of EAF1 was added to test its interaction with TRIM28, while 500 ng and 1 μg of DBC1 was used in the respective reactions to check if the presence of DBC1 affected TRIM28-EAF1 association. I. Western blot analyses showing the effect of DBC1 overexpression on degradation of endogenous EAF1 in TRIM28 knockdown cells when compared to control scramble cells. Cells depleted of TRIM28 cannot degrade EAF1 even in the presence of overexpressed DBC1. Quantification of EAF1 levels relative to actin are indicated.

TRIM28 is a ubiquitin E3 ligase for EAF1 and causes its degradation through ubiquitination. Next, we addressed whether TRIM28 would be able to degrade EAF1 within mammalian cells. Coexpression of both of these proteins within mammalian cells showed marked downregulation of EAF1 expression with concomitant expression of TRIM28 (Fig. 6A, compare lane 2 versus lane 3). This downregulation of expression can be rescued with addition of MG132 (Fig. 6A, compare lanes 3 versus lanes 4–6), thus further suggesting an involvement of ubiquitin proteasome-mediated degradation of EAF1 by TRIM28 within mammalian cells. Subsequent immunoprecipitation analysis clearly showed enhanced EAF1 ubiquitination upon coexpression of TRIM28 (Fig. 6B, compare lane 2 versus lanes 3). Addition of MG132 further increased this ubiquitination signal (Fig. 6B, compare lane 3 versus lane 4–6). Ubiquitin E3 ligase activity of TRIM28 is absolutely required for this EAF1 degradation since usage of ligase-deficient TRIM28 mutant (C65A, C68A) (29) failed to degrade EAF1, whereas the wild type (WT) showed efficient degradation (Fig. 6C, compare lane 2 with lanes 3–4 versus lanes 5–6). Consistent with its reduced degradation capability, the ligase-deficient TRIM28 also failed to ubiquitinate EAF1 when compared to WT (Fig. 6D, compare lane 2 with lanes 3–4 versus lanes 5–6). Consistent with a role of TRIM28 in regulating EAF1 stability, stable TRIM28 knockdown by multiple short hairpin RNAs (shRNAs) showed

enhanced expression of endogenous EAF1 within mammalian cells (Fig. 6E). Further, CHX chase assay showed that human EAF1 protein is fairly stable within the time points of our assay system (Fig. 6F, lanes 1–5). However, when compared to vector control, in the presence of overexpressed TRIM28, enhanced degradation kinetics of endogenous EAF1 was observed (Fig. 6F, compare lanes 1–5 versus lanes 6–10). These data clearly suggest that TRIM28 acts as a bona fide ubiquitin E3 ligase for EAF1 for controlling its stability within mammalian cells.

DBC1-mediated enhanced TRIM28 interaction with EAF1 is required for its degradation. Based on our observation that DBC1 interacts with TRIM28 and promotes EAF1 degradation, we hypothesized that DBC1 could enhance TRIM28 interaction with EAF1 and thus promote its degradation within mammalian cells. Since WT TRIM28 causes degradation of EAF1, we used the TRIM28 catalytic dead mutant (C65A, C68A) that failed to degrade EAF1 efficiently (Fig. 6C). As shown in Fig. 6G, immunoprecipitated FLAG-EAF1 interacted with ectopically expressed TRIM28 as observed earlier (Fig. 6G, lane 3). However, in the presence of overexpressed DBC1, EAF1 interaction with TRIM28 was markedly enhanced (Fig. 6G, compare lane 3 with lanes 4–6). For providing a direct evidence of this mechanism, we performed *in vitro* interaction analyses with purified proteins (Fig. S4G). As shown in Fig. 6H, purified GST-TRIM28 protein directly interacts with purified EAF1 (Fig. 6H, lane 6). This interaction is specific since in the same assay, GST alone failed to show any interaction with EAF1 (Fig. 6H, lane 2). Interestingly, and consistent with our observations within mammalian cells, addition of purified DBC1 markedly enhanced TRIM28 interaction with EAF1 (Fig. 6H, compare lane 6 with lanes 8–9). Based on these results, we conclude that human DBC1 enhances TRIM28 interaction with EAF1 both *in vitro* and *in vivo* within mammalian cells and thus could promote EAF1 degradation as observed in multiple assays.

Next, we addressed whether DBC1-mediated enhanced EAF1 interaction with TRIM28 would be a critical mechanism for EAF1 degradation. We analyzed DBC1 interaction with endogenous TRIM28 within mammalian cells by immunoprecipitation analyses and observed that deletion of the 795–923 amino acid region significantly reduced DBC1 interaction with TRIM28 (Fig. S4H, lane 3), whereas further deletion of 341–703 restored this interaction (Fig. S4H, lane 5) suggesting that the internal 341–703 region plays an inhibitory role in this overall DBC1 interaction with TRIM28. Deletion of the N-terminal S1-like RNA binding domain (1–111 amino acids) failed to show any effect on this interaction (Fig. S4H, lane 7). Interestingly, the TRIM28 interaction-defective DBC1 domain also failed to degrade endogenous EAF1 (Fig. S4I, compare lanes 2–3 with lanes 4–5), whereas the N-terminal-deleted 112–923 domain fully retained its capacity to degrade the EAF1 (Fig. S4I, compare lanes 2–3 with lanes 6–7). These experiments thus suggested a critical role of DBC1-TRIM28 interaction in degradation of EAF1 within mammalian cells. Further, consistent with this hypothesis, overexpression of DBC1 failed to degrade endogenous EAF1 upon TRIM28 knockdown (Fig. 6I, compare lanes 1–4 with lane 5–8).

Reciprocal regulation of DBC1 and EAF1 for maintaining ELL stability within mammalian cells. Since both DBC1 and EAF1 coregulate expression of each other, we were interested in addressing whether this mechanism of action is required for maintaining ELL stability within mammalian cells for expression of key target genes for cell survival. In our initial analyses, we generated stable DBC1 knockdown cells that also showed reduced expression of ELL and slightly enhanced expression of EAF1 protein level in the initial passages while maintaining the knockdown cells (Fig. 7A, lane 3). Interestingly, at the later passages, we were intrigued by observation that the ELL protein level was restored along with the increased expression of EAF1 protein (Fig. 7A, lanes 5–6). However, in that same stage, DBC1 protein level was relatively low. Subsequent mRNA analyses of cells harvested during these passages clearly showed that mRNA level of ELL and EAF1 proteins did not change significantly during these passages while DBC1 mRNA was maintained at low levels because of its knockdown by shRNA (Fig. 7B). These results thus suggest that the level of DBC1 and EAF1 proteins are reciprocally regulated during growth of mammalian cells such that optimal levels

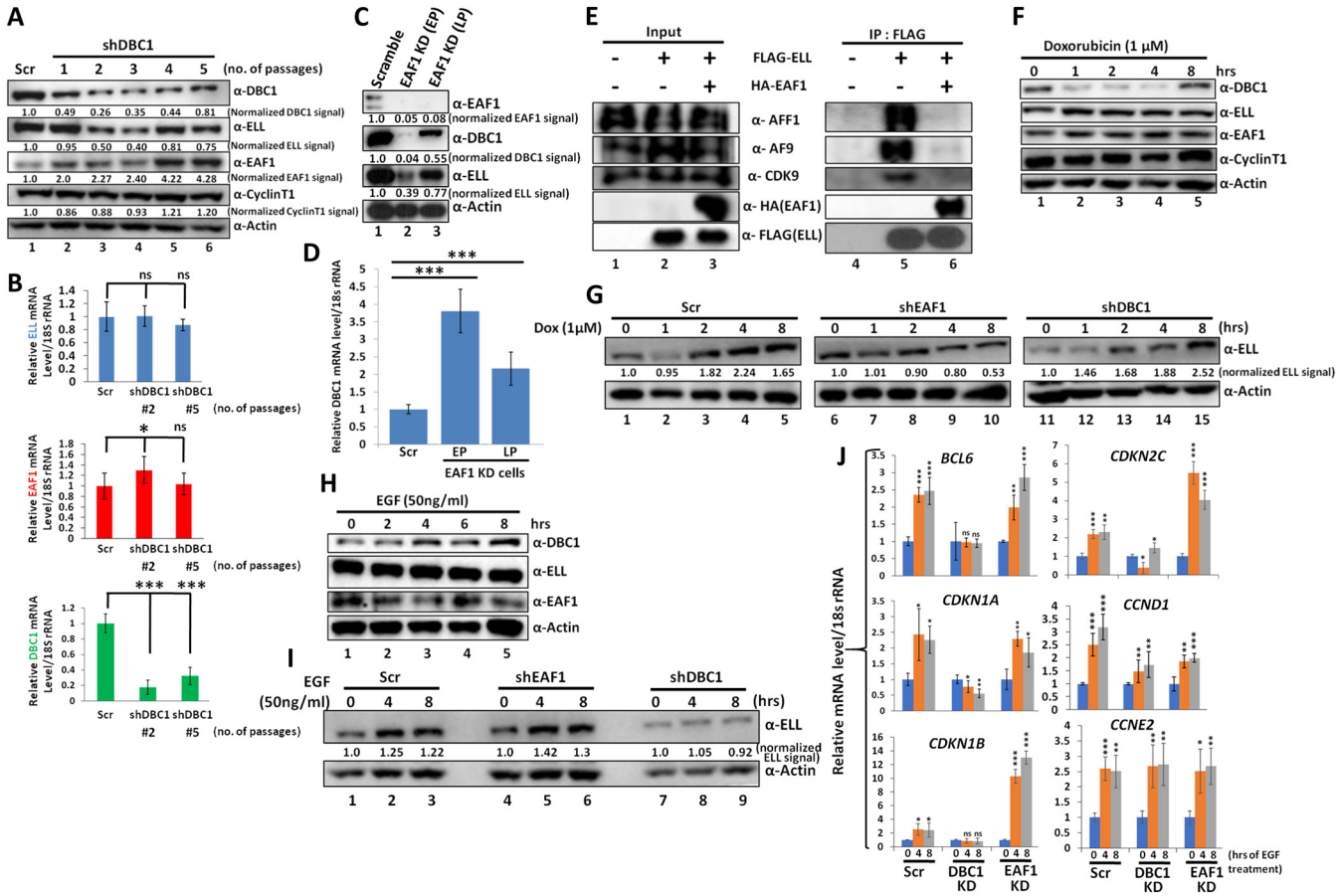

FIG 7 DBC1 and EAF1 regulate each other's levels in a context-dependent manner to maintain the cellular pool of ELL protein and its functions. (A) Western blot analyses showing the levels of indicated proteins in different passages of DBC1 knockdown cells compared to control scramble cells. ELL protein levels initially decrease upon DBC1 depletion but subsequently increase as EAF1 levels are enhanced in later passages/generations of cells. (B) qRT-PCR analyses showing the mRNA levels of ELL, EAF1, and DBC1 in different passages of DBC1 knockdown cells compared to control scramble cells. Both ELL (top panel) and EAF1 (middle panel) mRNA levels remained unaffected upon DBC1 knockdown. Value of each sample was normalized with 18s rRNA level that was used as an internal control. For calculation, mRNA levels normalized to 18s rRNA were further normalized to the value in control scramble cells to show their fold change. (C) Western blot analyses showing the levels of indicated proteins in different passages of EAF1 knockdown cells compared to control scramble cells (EP= early passage, LP= late passage). (D) qRT-PCR analyses showing the mRNA levels of DBC1 in early and late passages in EAF1 knockdown cells compared to control scramble cells. Value of each sample was normalized with 18s rRNA level that was used as an internal control. For calculation, mRNA levels normalized to 18s rRNA were further normalized to the value in control scramble cells to show their fold change. (E) Immunoprecipitation and subsequent Western blot analyses showing the effect of presence of EAF1 on ELL-SEC interaction. The overexpression of EAF1 greatly reduces ELL interaction with other SEC components such as AFF1, AF9, and CDK9. (F) Immunoblots showing changes in the levels of indicated proteins upon exposure to genotoxic stress by addition of Doxorubicin for different time periods in 293T cells. (G) Immunoblots showing changes in the levels of ELL protein upon exposure to genotoxic stress for different time periods in control scramble cells, EAF1 and DBC1 knockdown cells. (H) Western blot analyses showing changes in the levels of indicated proteins upon exposure to epidermal growth factor (EGF) for different time periods in 293T cells. (I) Immunoblots showing changes in the levels of ELL protein upon exposure to EGF for different time periods in control scramble cells, EAF1 and DBC1 knockdown cells. (J) qRT-PCR analyses showing the change in mRNA levels of indicated target genes in control scramble cells, DBC1 and EAF1 knockdown cells upon EGF treatment for different periods of time. Value of each sample was normalized with 18s rRNA level that was used as an internal control. For calculation, mRNA levels normalized to 18s rRNA were further normalized to the value in untreated (0 h) cells to show their fold change. In these experiments, qRT-PCR data represents as mean +/– SD. Student's *t* test was used to calculate the statistical significance of the data in this figure. *, $P \leq 0.05$; **, $P \leq 0.01$; and ***, $P \leq 0.001$. At least $n = 2$ biological replicates were performed for each experiment.

of key elongation factor ELL is maintained for proper expression of target genes for cell survival.

A reciprocal analysis with EAF1 knockdown also showed initial downregulation of expression of ELL protein with reduced expression of DBC1 (Fig. 7C, lane 2). However, at later passages while maintaining cells, we observed restoration of expression of ELL protein level with concomitant restoration of DBC1 expression (Fig. 7C, lane 3). Subsequent mRNA analyses showed that upon EAF1 knockdown, the DBC1 mRNA level was significantly upregulated and remained so for the subsequent late passages that we have tested (Fig. 7D, compare scramble versus EP and LP lanes). These data are consistent with our initial observation wherein overexpression of EAF1 reduced

endogenous DBC1 mRNA expression within mammalian cells in a dose-dependent manner (Fig. 5C). All these analyses clearly indicate that under normal physiological growth conditions, mammalian cells adapt themselves through modulation of expression of key regulatory components for optimal expression of genes that are important for survival and proliferation of cells.

A recent study has shown a negative role of human EAF1 and EAF2 in SEC formation that appears to be important for transcription from the HIV LTR promoter (30). Consistent with this report, we have also observed a negative role of human EAF1 in ELL interaction with other SEC components such as CDK9, AF9, and AFF1 (Fig. 7E). These results thus indicate that EAF1-mediated negative regulation of SEC formation could play an important role in DBC1 transcription within mammalian cells as observed in our assays (Fig. 5C and Fig. 7C–D), whereas maintenance of overall ELL level is key for expression of diverse target genes (Fig. 4 and Fig. S3). Further in-depth studies would be required for clarifying the overall functional regulation. Nevertheless, identification of reciprocal coregulation of DBC1 and EAF1 proteins in maintaining ELL protein level within mammalian cells by two different mechanisms (as discussed) is certainly a major advancement in our overall understanding of ELL and thus SEC-mediated transcriptional regulation for expression of diverse sets of genes within mammalian cells.

Context-dependent maintenance of ELL protein level by DBC1 and EAF1 within mammalian cells. Based on our observation that knockdown of either DBC1 or EAF1 results in increased expression of other factors for maintaining ELL protein level, we wondered whether this mechanism of coregulation would be involved in context-dependent physiological responses within mammalian cells. Little elongation complex (LEC) has been shown to be required for transcriptional restart after repair of damaged DNA upon exposure to genotoxic stress (31). Thus, we hypothesized that EAF1-mediated maintenance of ELL level would be a key functional response during exposure to genotoxic stress. Consistent with this hypothesis, we were intrigued to observe reduced DBC1 expression within mammalian cells upon exposure to doxorubicin (Fig. 7F and Fig. S5A, DBC1 panel) that predominantly causes DNA damage through inhibition of functions of topoisomerase II. Interestingly, in this same treatment, we also observed modest but reproducible increased expression of EAF1 protein that resulted in increased expression of ELL protein as well (Fig. 7F and Fig. S5A, EAF1 and ELL panels). The overall increase in ELL protein level is indeed dependent on increased EAF1 expression since EAF1 knockdown cells failed to show enhanced ELL expression when compared to control scramble cells (Fig. 7G, compare lanes 1–5 with lanes 6–10) upon doxorubicin treatment. However, in the same assay, DBC1 knockdown resulted in enhanced expression of ELL (Fig. 7G, compare lanes 1–5 with lanes 11–15). These results thus suggested EAF1-dependent enhanced ELL expression is a context-dependent physiological response of mammalian cells upon exposure to genotoxic stress. Reduced DBC1 expression upon doxorubicin treatment lead to enhanced EAF1 expression, thus causing increased abundance of LEC that is required for optimal transcriptional restart after repair of damaged DNA as reported earlier (31).

Next, we hypothesized that the DBC1-mediated maintenance of ELL level could be involved in proper cellular functions during conducive growth and proliferation condition. To address this, we treated the cells with epidermal growth factor (EGF) and checked the level of expression of target proteins at different time points after treatment. Intriguingly, treatment with EGF markedly enhanced expression of DBC1 protein level while concomitantly reducing expression of EAF1 protein (Fig. 7H and Fig. S5B, compare DBC1 with EAF1 panels). Concomitantly, we have also observed a modest increase in ELL protein level (Fig. 7H and Fig. S5B). The increased expression of ELL is dependent on the presence of DBC1 since its knockdown fails to increase ELL protein level, whereas, the EAF1 knockdown shows a modest but reproducible enhancement (Fig. 7I compare lanes 1–3 with lanes 4–6 and 7–9). These results thus further suggested presence of a negative feedback loop mechanism between DBC1 and EAF1 (as representative of EAF1 and EAF2) in maintenance of key elongation factor ELL within mammalian cells for context-dependent response for cellular functions.

TABLE 1 Plasmids used in this study

Name of Plasmid	Description	Source
M10	FLAG-HA pCDNA5-FRT-TO vector	(8)
M13	AF9 cloned into FLAG-HA pCDNA5-FRT-TO vector	(8)
M15	ELL cloned into FLAG-HA pCDNA5-FRT-TO vector	(8)
M24	AFF1 cloned into FLAG-HA pCDNA5-FRT-TO vector	(8)
M56	pET-GST vector	GE Amersham
M61	ELL cloned into pET-GST vector	(13)
M237	EAF1 cloned into FLAG-HA pCDNA5-FRT-TO vector	(8)
M238	EAF2 cloned into FLAG-HA pCDNA5-FRT-TO vector	(8)
M250	CDK9 cloned into FLAG-HA pCDNA5-FRT-TO vector	(8)
M296	psPAX2 lentivirus packaging plasmid	Addgene plasmid#12260
M297	pMD2.G lentivirus envelope plasmid	Addgene plasmid#12259
M298	Lentiviral pLKO.1 vector containing scramble sequence (control for shRNA knockdown)	(13)
M336	DBC1 cloned into FLAG-HA pCDNA5-FRT-TO vector	(24)
M428	EAF1 (1–208) fragment cloned into FLAG-HA pCDNA5-FRT-TO vector	(13)
M429	EAF1 (1–148) fragment cloned into FLAG-HA pCDNA5-FRT-TO vector	(13)
M430	EAF1 (1–88) fragment cloned into FLAG-HA pCDNA5-FRT-TO vector	(13)
M431	EAF1 (61–268) fragment cloned into FLAG-HA pCDNA5-FRT-TO vector	(13)
M432	EAF1 (121–268) fragment cloned into FLAG-HA pCDNA5-FRT-TO vector	(13)
M433	EAF1 (181–268) fragment cloned into FLAG-HA pCDNA5-FRT-TO vector	(13)
M434	EAF1 cloned into pET-GST vector	(13)
M435	EAF1 cloned into 6xHis-pET-11d vector	This study
M455	EAF1 cloned into FLAG pCDNA5-FRT-TO vector	(13)
M458	EAF2 cloned into FLAG pCDNA5-FRT-TO vector	(13)
M464	DBC1 cloned into FLAG pCDNA5-FRT-TO vector	(24)
M465	DBC1 cloned into HA pCDNA5-FRT-TO vector	(24)
M499	EAF1 cloned into pEGFP-N2 vector	This study
M580	AFF4 cloned into FLAG-HA pCDNA5-FRT-TO vector	(25)
M742	ELL (1–500) fragment cloned into FLAG pCDNA5-FRT-TO vector	(24)
M743	ELL (1–373) fragment cloned into FLAG pCDNA5-FRT-TO vector	(24)
M744	ELL (45–621) fragment cloned into FLAG pCDNA5-FRT-TO vector	(24)
M745	ELL (374–621) fragment cloned into FLAG pCDNA5-FRT-TO vector	(24)
M746	ELL (45–373) fragment cloned into FLAG pCDNA5-FRT-TO vector	(24)
M747	ELL cloned into FLAG pCDNA5-FRT-TO vector	(24)
M758	DBC1 (1–794) fragment cloned into FLAG-HA pCDNA5-FRT-TO vector	(24)
M759	DBC1 (1–704) fragment cloned into FLAG-HA pCDNA5-FRT-TO vector	(24)
M760	DBC1 (1–340) fragment cloned into FLAG-HA pCDNA5-FRT-TO vector	(24)
M761	DBC1 (1–243) fragment cloned into FLAG-HA pCDNA5-FRT-TO vector	(24)
M762	DBC1 (112–923) fragment cloned into FLAG-HA pCDNA5-FRT-TO vector	(24)
M792	HDAC3 cloned into FLAG pCDNA3.1 vector	Addgene plasmid #13819
M912	Ubiquitin cloned into EGFP-C1 vector	Addgene plasmid#11928
M993	ELL (61–621) fragment cloned into pET-GST vector	(24)
M998	EAF1 (1–208) fragment cloned into pET-GST vector	This study
M999	EAF1 (1–148) fragment cloned into pET-GST vector	This study
M1000	EAF1 (1–88) fragment cloned into pET-GST vector	This study
M1001	EAF1 (61–268) fragment cloned into pET-GST vector	This study
M1002	EAF1 (121–268) fragment cloned into pET-GST vector	This study
M1003	EAF1 (181–268) fragment cloned into pET-GSTvector	This study
M1028	TRIM28 cloned into pKH vector	Addgene plasmid #45569
M1029	TRIM28 catalytic dead mutant (C65A/C68A) cloned into pKH vector	Addgene plasmid #92199
M1156	ELL cloned into 6xHis-pET-11d-GFP vector	This study
M1256	EAF1 cloned into 6xHis-pET-11d-RFP vector	This study

Since in our assays, we have observed increased expression of DBC1 and concomitant ELL proteins upon EGF treatment during late time points, we presumed that this response could be important for expression of EGF-induced late response genes. Indeed, expression of some of the late response genes, that we have tested, are increased upon EGF treatment in control scramble cells. However, similar analysis using DBC1 knockdown cells that have undergone multiple passages, where ELL levels are restored to normal by increased expression of EAF1, failed to induce expression of

TABLE 2 shRNA constructs used for making stable knockdown cells

Name of Plasmid	Description	Sequence
S35	DBC1 shRNA #4 cloned into pLKO.1 puro vector	CCGGGCCAAAGGAAAGGATCTCTTTCTCGAGAAAGAGATCCTTTCCTTTGGCTTTTTG
S41	EAF1 shRNA cloned into pLKO.1 puro vector	CCGGGAACACCCTCAGAAATGACTTCTCGAGAAGTCATTTCTGAGGGTGTTCTTTTTG
S46	EAF2 shRNA cloned into pLKO.1 puro vector	CCGGGTGACCATAACTCTGCCAAATCTCGAGATTTGGCAGAGTTATGGTCACTTTTTG
S152	TRIM28 shRNA#1 cloned into pLKO.1 puro vector	CCGGCCTGGCTCTGTTCTCTGTCCTCTCGAGAGGACAGAGAACAGAGCCAGGTTTTT
S153	TRIM28 shRNA #2 cloned into pLKO.1 puro vector	CCGGGAGAATTATTTCATGCGTGATCTCGAGATCACGCATGAAATAATTCTCTTTTT
S154	TRIM28 shRNA #3 cloned into pLKO.1 puro vector	CCGGGAGGACTACAACCTTATTGTTCTCGAGAACAATAAGGTTGTAGTCCTCTTTTT
S155	TRIM28 shRNA #4 cloned into pLKO.1 puro vector	CCGGCTGAGACCAAACCTGTGCTTACTCGAGTAAGCACAGGTTTGGTCTCAGTTTTT
S156	TRIM28 shRNA #5 cloned into pLKO.1 puro vector	CCGGGACCACCAGTACCAGTTCTTACTCGAGTAAGAACTGGTACTGGTGGTCTTTTT
S157	TRIM28 shRNA #6 cloned into pLKO.1 puro vector	CCGGGCACTAGCTGTGAGGATAATGCTCGAGCATTATCCTCACAGCTAGTGCTTTTT

these genes (Fig. 7J), whereas EAF1 knockdown cells at a similar stage showed either equal or increased induction compared to control scramble cells (Fig. 7J).

Thus, our results in this study decipher previously unidentified roles of several players that coordinately regulate each other for maintaining the overall level of a key elongation factor ELL (that are part of both SEC and LEC) within mammalian cells. This study thus emphasizes the prevailing complexity within mammalian cells for protecting important factors that is absolutely essential for context-dependent physiological response and cell survival.

DISCUSSION

Overall, our results in this study have shown novel roles of human EAF1 and EAF2 in regulating ELL stability within mammalian cells through competitive binding with HDAC3 at the N terminus of ELL, thus protecting it from deacetylation and subsequent ubiquitin proteasome-mediated degradation. Since DBC1 also plays a similar role in regulating ELL stability, our further in-depth analyses identified presence of important negative feedback loop mechanisms between EAF1 and DBC1 for protecting ELL stability for survival of cells as well as context-dependent physiological response of mammalian cells. The overall mechanism of action, as identified by our studies, is presented in Fig. S5C.

Although elongation functions of ELL in transcriptional regulation have been appreciated, the overall temporal regulation of transcription through modulation of its abundance is completely unknown. In this context, it is essential to understand the factors regulating stability of ELL. Our earlier study has shown coordination of multiple factors in regulating ELL stability and thus its function for expression of target genes (24). Apart from finding a novel role of EAF1 and EAF2 in regulating ELL stability and its functions, our study further extends the cross talk between two factors, namely, DBC1 and EAF1, that employ similar mechanism of action in overall regulation of ELL stability and thus its functions.

From our studies, we have clearly shown the role of the N-terminal domain of ELL in factor binding for regulation of its stabilization. Earlier studies have shown the role of C-terminal domain of ELL in SEC interaction (28). Therefore, it is getting increasingly clear that ELL has two nonoverlapping domains that mediate two separate functions — the N-terminal domain for regulation of its stability and C-terminal domain for SEC association.

Apart from being a component of SEC, ELL is also a part of LEC, in association with EAF1, that plays an essential role in snRNA biogenesis (32, 33). LEC has also been shown to play an important role in transcriptional recovery after DNA repair (31). Our study points toward a unique role of EAF1 in stabilizing ELL during exposure to genotoxic stress and not during conducive growth conditions. This could be highly possible as an example of adaptive response of mammalian cells for transiently protecting key factor(s) that would be required for immediate downstream responses. Interestingly, this response is specific as evidenced from our analyses that a different cellular

response occurs upon exposure to EGF, wherein DBC1-mediated ELL stability played important roles in regulating expression of late-induced genes.

There are few instances wherein feedback loop mechanisms have been described in direct functional regulation between two different factors, including p53 (34). However, to our knowledge, existence of feedback loop mechanisms between two factors for controlling functions of a third factor has not been described. Further and importantly, the functional regulation of a key transcriptional elongation factor by two other factors, involved in controlling its overall stability by similar mechanisms, has not been described. Therefore, our study paves the way for molecular understanding of overall functional regulation of key factors within mammalian cells by other regulators that perform similar functions through identical mechanisms.

The effect of EAF1 and EAF2 on ELL stabilization could have potential implications in mixed lineage leukemia (MLL) fusion protein-mediated leukemogenesis as well. It is interesting to note that the MLL-EAF1 fusion protein can also transform the lineage-negative mouse progenitor cells, as has been shown by an earlier study (35). It could be highly possible that the overexpression of derived MLL-EAF1 fusion protein can increase overall ELL level and thus increase other target gene expression required for leukemogenesis. Also, our studies further point toward a key role of human DBC1 in regulating SEC functions and thus its potential role in regulation of MLL fusion protein-mediated leukemogenesis. Further studies would be needed for detailed understanding of the role of EAF1 and EAF2 in overall regulation of MLL fusion-mediated leukemogenesis.

MATERIALS AND METHODS

Cell culture and transfection. All cell lines used in this study were cultured and maintained in Dulbecco's modified Eagle medium DMEM (Invitrogen, USA) supplemented with fetal bovine serum (FBS) (Gibco, USA) [final concentration 10%], along with 100 U/mL penicillin-streptomycin (Life Technologies, USA). Transfections were performed using Fugene transfection reagent (Promega) as per manufacturer's protocol. Cells were harvested 48 h posttransfection for downstream analyses, unless otherwise mentioned.

Plasmids, primers and antibodies. All the plasmids used for this study, primers used for RNA and ChIP analyses, construction of shRNAs, and antibodies used for various experiments are mentioned in Tables 1–4.

Generation of different expression constructs. Plasmid constructs containing the cDNA sequences of AFF1, AF9, CDK9, ELL, EAF1, and EAF2 were purchased from Open Biosystems, USA and were subsequently cloned into desired expression vectors. The HDAC3 expression plasmid was obtained from Addgene. The cDNA sequences were then cloned into epitope tag-containing pcDNA5/FRT/TO plasmids (Thermo Fisher Scientific, USA) for expression in mammalian cells. For the purpose of cloning different deletion mutants, target sequences were amplified using appropriate primers and cloned into the pcDNA5/FRT/TO plasmid. For bacterial expression, cloning was performed in 6×His pET-11d for His-tagged proteins and pET-GST vector for GST tagging. Site directed mutagenesis was done using the QuikChange II site-directed mutagenesis kit (Agilent Technologies, USA). The corresponding author of this study may be contacted for further details of all the clones that have been generated for the purpose of this study.

Purification of recombinant proteins. Purification of recombinant proteins was carried out from *E. coli* BL21 (DE3) or HEK-293T cells. For bacterial expression and purification, *E. coli* BL21(DE3) cells transformed with the expression vector of interest were grown in LB containing required antibiotic and induced with 1 mM isopropyl-β-D-thiogalactopyranoside (IPTG) (GoldBio, USA) for 4 h at 37°C in an orbital shaker. Cells were harvested and lysed by sonication (60% amplitude, alternating between 30-s on and off cycles, for 10 min). The separated supernatant was incubated with glutathione-agarose beads for GST-tagged proteins and Ni-NTA beads for His-tagged proteins. After incubation with beads for 4 h, the supernatant was removed, and beads washed extensively with appropriate buffers. Elution, if required, was performed with His elution buffer containing 250 mM imidazole or GST elution buffer containing 30 mM L-GST peptide (Sigma-Aldrich) in 100 mM Tris-Cl buffer.

In case of mammalian expression and purification, 293T cells were transfected with plasmids expressing the protein of interest. At 48 h posttransfection, cells were harvested and lysed in BC1000 buffer (20 mM Tris-Cl; pH 8.0; 1,000 mM KCl; 2 mM EDTA; 20% glycerol). Immunoprecipitation was performed as described below. For elution of proteins, washed beads were incubated with 3X-FLAG peptide (150 ng/μL final concentration) for 1 h. Purification of proteins was assayed by SDS-PAGE followed by Coomassie staining.

Immunoprecipitation analyses. In case of ectopically expressed epitope-tagged proteins, cells were harvested 48 h posttransfection and lysis was carried out in BC150 buffer (20 mM Tris-Cl, pH 8.0, 150 mM KCl, 2 mM EDTA, 20% glycerol), unless otherwise mentioned. Next, 100 μg of the total protein lysate was incubated with prewashed anti-FLAG M2 agarose beads (Sigma, USA) or anti-HA agarose beads (Sigma, USA) as per the experimental design for 12 h at 4°C and continuous rotation at 16 rpm for

TABLE 3 Primers used for RNA analysis

Primer name	Forward primer sequence	Reverse primer sequence
GAPDH	CATCACCATCTTCCAGGAG	GTTCACACCCATGACGAAC
18srRNA	GTAACCCGTTGAACCCCATT	CCATCCAATCGGTAGTAGCG
AFF1	GAATTCTTTGCTCGGCTCAGCAC	CTTGTAGCTGCTGAAAACCCTGTC
AFF4	GGATAAAGTAATGGGCCCTCTCATC	TCAAGATATCAACTTGGCATCCTGG
AF9	GGTGAATGTGACAAGGCATACCTAG	GGTTTTGTCCAGCGAGCAAAGATC
CDK9	GCATCATGGCAGAGATGTG	GTTGTCCACGTTTGGCC
DBC1	GAGGAGTTTGCAGGAGC	GTAGCCACACCAGTTGG
ELL	GACCAACACCAACTACAGCCAGG	GTACTCGGCGATGAGCCTCTTG
EAF1	CGTTGCCAATGGAACCAGCC	CATCACTGTCACTGCCAGACTC
EAF2	GTGTCTCAGGACATCCTACCATG	CATCAGAAGGCCACTGTTGTCTC
BARX2	AGCTCAAAGCAGCCAG	GTGATCACCGAGAGGAG
BCL6	CCACACAGGAGAGAAACCTTAC	GCAGGTCAGTGGCTGACAC
CBX4	CTGGTCGCCCAAATATAAC	TCAGGACATTGGAACGAC
CCND1	TCTAAGATGAAGGAGACCAT	GGAAGTGTTCAATGAAATCG
CCNE2	GCTGGCCTATGTGACTTACC	GGTAGACTTCGATGGGCCC
CDK6	GGAGTGTTGGCTGCATATTTG	CGATATCTGTTACAAACTTC
CNN3	CTACAGAACCTGTCATTC	ATCTCTGGGGTAGTCATC
DCAF4	AAACCTCTACTTCACCAACC	CTGGGTGACTATTGACGAA
DDB2	TACCCCTTATGAATTGAGG	CAGATGAGAATGTGGTAAC
KIF1A	AGAAGGTGAGCAAAATCAG	CGGAATGAAATCTGTCTTC
KIF1B	AATCAGAGTGACTTTTCGTC	ATTCGACTGATTTCTTCTGG
MDM2	TTGGATCAGGATTCAGTTTC	GAGAGTTCTTGTCCTTCTTC
MED15	GACCTTTAAACACACCTGTG	GGCTCTTCATCTTACTCAGG
Myo10	CTTCAGGATGAGGCCATC	GCCAGCTGTACAGGTTG
NFKB2	GAGAACGGAGACACACC	CAGAAAGCTCACCACAC
SKI	CCAAGTACTCGGCCCAGATC	GCACGGAATCTACGGCTCC
TAF6	CTTGCTGAAGGTTCCTG	GAAGTGGTGGTGGAAC
ZFX	CATAGATGAGTCTGCTGGC	CCTCTCGACTTAAACTTCTTC
E2F2	GGAGCCGGACAGTCCTTC	GCTGTCAGTAGCCTCCAAG
CDKN1A	GGACAGCAGAGGAAGACCATG	CTGTCATGCTGGTCTGCC
CDKN1B	CGACGATTCTTCTACTCAA	TTACGTTTGACGTCTTCTG
CDKN1C	GCTGCACTCGGGGATTTC	GGACATCGCCCGACGACT
CDKN2C	GGATTTGGAAGGACTGCG	GCTTGAAACTCCAGCAAAGTC
Myc	GCTTGTACCTGCAGGATC	GACTCCGTCGAGGAGAG
SMAD2	GCAGAGCCCCAATTGTAATC	GGTGCACATTCTAGTTAGCTG
MCL1	CGTAAGGACAAAACGGGAC	GGTGGTTGGTTAAAAGTCAAC
BMI1	GGAGGAGGTGAATGATAAAAG	CCATTCCTTCTCCAGGTAT
BMP2	CCAGACCACCGGTTGGAG	GCTCTGCTGAGGTGATAAACTC
APOE	GCGGATGGAGGAGATG	CTCGAACCAGCTCTTG
PCNA	GGAGGAAGCTGTTACCATAGAG	CCTCGATCTTGGGAGCCAAG
RGS2	AAGATTGGAAGACCCGTTTGAG	GCAAGACCATATTTGCTGGCT
VDAC1	CAAGTATCAGATTGACCCTG	GTCAGTTTAATACCTGGC
WEE1	GCTGTCCGCTTCTAGAAAG	CGAGATGTTCTATTACTCTGGG
HOAX13	CCTTGGGTCTTCCCATGGAAA	CCTCCTATAGGAGCTGGCATC
MEF2D	GACCTGAACAGTGCTAACG	GTGATGACTCGCAGGTC
VPS29	GCATATAATGCCTTGGAAAC	CACATCATCTCCAATTAGC

immunoprecipitation of the tagged proteins. The beads were then washed rigorously with BC150 buffer containing 0.1% NP-40 to remove unbound proteins and finally boiled in 1 × SDS loading dye at 95°C for 5 min for eluting bead-bound proteins. Eluted proteins were analyzed by SDS-PAGE followed by Western blotting. For analyzing posttranslational modifications, lysis and immunoprecipitation was performed in BC1000 buffer (20 mM Tris-Cl, pH 8.0, 1M KCl, 2 mM EDTA, 20% glycerol). In these experiments as well, the immunoprecipitation buffer was supplemented with 0.1% NP-40 for washing unbound proteins.

***In vitro* interaction analyses.** For *in vitro* interaction analyses, the bait proteins were immobilized on agarose beads, whereas the prey proteins were added in solution. After incubation in appropriate buffer, the bead-bound proteins were centrifuged briefly, and the supernatant was discarded to remove unbound proteins. The beads were then washed thrice with wash buffer (20 mM Tris-Cl, pH 8.0, 100 mM KCl, 2 mM EDTA, 20% glycerol, 0.1% NP-40) and bound proteins were eluted by boiling in 1 × SDS loading dye at 95°C for 10 min. Protein samples were loaded on SDS-PAGE and were subsequently analyzed by immunoblotting.

TABLE 4 Antibodies used in this study

Name of factor	Source
FLAG epitope tag	Sigma
β-actin	Santa Cruz Biotechnology
GST	Santa Cruz Biotechnology
GFP	Biobharati Life Science
Ubiquitin	Cell Signaling Technology
His tag	Santa Cruz Biotechnology
HA tag	Santa Cruz Biotechnology
EAF1	Santa Cruz Biotechnology
EAF2	Bethyl Lab and Cell Signaling Technology
ELL	Bethyl Lab and Cell Signaling Technology
AFF1	Abcam
AF9	Bethyl Lab
CyclinT1	Santa Cruz Biotechnology
CDK9	Santa Cruz Biotechnology
DBC1	Cell Signaling Technology
Acetyllysine	Cell Signaling Technology
p300	Cell Signaling Technology
TRIM28	Cell Signaling Technology

Western blotting. For most of the experiments, Western blotting was used to detect target proteins, and/or the interactions between them. Analysis of protein levels from whole-cell extracts (input samples) involved mixing of the samples with 5X Laemmli buffer (312.5 mM Tris, 250 mM SDS, 50% glycerol, 25% β-Mercaptoethanol, and bromophenol blue as an indicator) and boiling for 5 min at 95°C. In case of immunoprecipitation or *in vitro* interaction reactions, wherein target proteins remained immobilized on the beads/agarose resin used, the proteins were eluted by addition of 1X Laemmli buffer (62.5 mM Tris, 50 mM SDS, 10% glycerol, 5% β-Mercaptoethanol, and bromophenol blue as indicator) and boiling the mixture for 5 min at 95°C. Loading of input samples varied between 2.5 and 5% depending on the abundance of the target protein. In case of immunoprecipitation/posttranslational modifications/*in vitro* interactions, loading of the eluted proteins varied between 10 and 30% depending on the target and strength of interaction between the bait and prey. Proteins were resolved by SDS-PAGE and subsequently transferred onto a nitrocellulose membrane (Bio-Rad, USA). Blocking was performed for 1 h at room temperature with 5% skim milk suspension in phosphate-buffered saline + 0.1% Tween 20 (PBST). Incubation with primary antibodies was carried out for 12 h at 4°C. Following this, the membrane was washed thrice with PBST and incubated with HRP conjugated antirabbit (Bio-Rad, USA) or antimouse (Cell Signaling Technology, USA) secondary antibodies for 1 h. Protein bands were visualized on the iBright imaging system (ThermoFisher, USA) after addition of Clarity Western ECL substrate (Bio-Rad, USA). All the immunoblots shown in this study represent a minimum of $n = 2$ biological replicates.

Cycloheximide (CHX) chase assay. For ectopically expressed proteins, cells were transfected with the indicated plasmids as mentioned. 24 h posttransfection, cycloheximide (Sigma, USA) was added to each well at a concentration of 100 μg/mL. For endogenous proteins, 36 h posttransfection, cycloheximide (Sigma, USA) was added to each well at a concentration of 100 μg/mL. At the respective time points, cells were harvested in ice cold PBS and lysed in RIPA buffer. Cell lysates were subjected to SDS-PAGE and analyzed by Western blotting using factor-specific or epitope tag-specific antibodies.

Generation of stable knockdown cell line. For the purpose of generating individual stable knockdown cells, specific shRNAs were cloned into pLKO.1 vector. In each well of a 6-well plate, 500 ng of a shRNA-encoding plasmid along with 375 ng of psPAX2 packaging plasmid and 125 ng of pMD2.G VSV-G envelope plasmid were transfected. At 24 h after transfection, old media were replaced by fresh media in each well and after 72 h, media containing virus particles was collected, centrifuged briefly, and used to transduce fresh cells at a confluence level of ~30 to 40%. To enhance viral transduction, Polybrene (8 μg/mL) was added. Then, 24 h after virus transduction, media was replaced with fresh media. The next day, cells were subjected to puromycin (3 μg/mL) selection. Selected cells were amplified and checked for the knockdown efficiency by RNA analysis through qRT-PCR and protein analysis by Western blots. The confirmed knockdown cells were used for further downstream assays.

To make the EAF1/EAF2 double knockdown cell line, an EAF2 knockdown cell line was generated initially as mentioned above. This EAF2 knockdown cell line was subsequently transduced with EAF1 shRNA containing virus using similar to the strategy mentioned above for making the stable EAF1/2 double knockdown cell line.

RNA extraction and qRT-PCR analysis. Total RNA was extracted from cells using TRIzol (Invitrogen) as per manufacturer's protocol. Then, 1 μg of total RNA was used for cDNA synthesis using a Verso cDNA synthesis kit (Thermo Scientific) following manufacturer's protocol. cDNA was diluted 50 times before using for qRT-PCR analysis. qRT-PCR was performed in CFX96 real-time PCR detection system

(Bio-Rad, USA) using iTaq universal SYBR green supermix (Bio-Rad, USA) and target gene-specific primers as mentioned in Table 3. Target gene expression level was normalized with either GAPDH or 18S rRNA that were used as internal control.

Mass spectrometry analysis. The mass spectrometry analysis for identifying DBC1-associated proteins has been described in detail in our earlier studies (14).

Colony formation assay. 1.5×10^4 cells were seeded in each well of a 6-well plate for colony formation assay. After 7 to 14 days, cells were fixed using fixing solution containing methanol: acetic acid (3:1) for 10 min at room temperature. Subsequently, colonies were stained using 0.5% crystal violet solution (in methanol) for 15 min. Colonies were washed with water multiple times until the excessive stain was removed.

Cell proliferation assay. 6×10^4 cells were seeded in each well of a 24-well plate for cell proliferation assay. The number of cells was counted using a hemocytometer on indicated days. In case of EAF1/2 double knockdown cells in which ELL expression was restored through its overexpression, cells were seeded 48 h after transfection and were counted on the indicated days.

Data availability. The full set of original raw images of western blots that were used for making the figures as described in this study can be accessed from Mendeley data repository through accessing the link https://data.mendeley.com/datasets/s3pzywyn9k.

SUPPLEMENTAL MATERIAL

Supplemental material is available online only.

SUPPLEMENTAL FILE 1, PDF file, 1.4 MB.

ACKNOWLEDGMENTS

This work was supported by a Wellcome-Trust DBT Intermediate Fellowship (IA/I/14/1/501287) awarded to D.B.; A.N., M.K.B., and S.P. are recipients of CSIR Fellowships; and S.B. is a recipient of a UGC Fellowship.

S.B. and A.N. performed majority of the experiments in consultation with D.B.; M.B. and S.P. also contributed to a few key experiments. A.N., S.B., and D.B. discussed the results and wrote the manuscript.

We declare no conflict of interest.

REFERENCES

1. Adelman K, Lis JT. 2012. Promoter-proximal pausing of RNA polymerase II: emerging roles in metazoans. Nat Rev Genet 13:720–731. https://doi.org/10.1038/nrg3293.
2. Williams LH, Fromm G, Gokey NG, Henriques T, Muse GW, Burkholder A, Fargo DC, Hu G, Adelman K. 2015. Pausing of RNA polymerase II regulates mammalian developmental potential through control of signaling networks. Mol Cell 58:311–322. https://doi.org/10.1016/j.molcel.2015.02.003.
3. Core L, Adelman K. 2019. Promoter-proximal pausing of RNA polymerase II: a nexus of gene regulation. Genes Dev 33:960–982. https://doi.org/10.1101/gad.325142.119.
4. Zhou Q, Li T, Price DH. 2012. RNA polymerase II elongation control. Annu Rev Biochem 81:119–143. https://doi.org/10.1146/annurev-biochem-052610-095910.
5. He N, Liu M, Hsu J, Xue Y, Chou S, Burlingame A, Krogan NJ, Alber T, Zhou Q. 2010. HIV-1 Tat and host AFF4 recruit two transcription elongation factors into a bifunctional complex for coordinated activation of HIV-1 transcription. Mol Cell 38:428–438. https://doi.org/10.1016/j.molcel.2010.04.013.
6. Lin C, Smith ER, Takahashi H, Lai KC, Martin-Brown S, Florens L, Washburn MP, Conaway JW, Conaway RC, Shilatifard A. 2010. AFF4, a component of the ELL/P-TEFb elongation complex and a shared subunit of MLL chimeras, can link transcription elongation to leukemia. Mol Cell 37:429–437. https://doi.org/10.1016/j.molcel.2010.01.026.
7. Yokoyama A, Lin M, Naresh A, Kitabayashi I, Cleary ML. 2010. A higher-order complex containing AF4 and ENL family proteins with P-TEFb facilitates oncogenic and physiologic MLL-dependent transcription. Cancer Cell 17:198–212. https://doi.org/10.1016/j.ccr.2009.12.040.
8. Biswas D, Milne TA, Basrur V, Kim J, Elenitoba-Johnson KS, Allis CD, Roeder RG. 2011. Function of leukemogenic mixed lineage leukemia 1 (MLL) fusion proteins through distinct partner protein complexes. Proc Natl Acad Sci U S A 108:15751–15756. https://doi.org/10.1073/pnas.1111498108.
9. Basu S, Nandy A, Biswas D. 2020. Keeping RNA polymerase II on the run: functions of MLL fusion partners in transcriptional regulation. Biochim Biophys Acta Gene Regul Mech 1863:194563. https://doi.org/10.1016/j.bbagrm.2020.194563.
10. Peng J, Zhu Y, Milton JT, Price DH. 1998. Identification of multiple cyclin subunits of human P-TEFb. Genes Dev 12:755–762. https://doi.org/10.1101/gad.12.5.755.
11. Price DH. 2000. P-TEFb, a cyclin-dependent kinase controlling elongation by RNA polymerase II. Mol Cell Biol 20:2629–2634. https://doi.org/10.1128/MCB.20.8.2629-2634.2000.
12. Takahashi H, Parmely TJ, Sato S, Tomomori-Sato C, Banks CA, Kong SE, Szutorisz H, Swanson SK, Martin-Brown S, Washburn MP, Florens L, Seidel CW, Lin C, Smith ER, Shilatifard A, Conaway RC, Conaway JW. 2011. Human mediator subunit MED26 functions as a docking site for transcription elongation factors. Cell 146:92–104. https://doi.org/10.1016/j.cell.2011.06.005.
13. Yadav D, Ghosh K, Basu S, Roeder RG, Biswas D. 2019. Multivalent role of human TFIID in recruiting elongation components at the promoter-proximal region for transcriptional control. Cell Rep 26:1303–1317.e7. https://doi.org/10.1016/j.celrep.2019.01.012.
14. Ghosh K, Tang M, Kumari N, Nandy A, Basu S, Mall DP, Rai K, Biswas D. 2018. Positive regulation of transcription by human ZMYND8 through its association with P-TEFb complex. Cell Rep 24:2141–2154.e6. https://doi.org/10.1016/j.celrep.2018.07.064.
15. Rahl PB, Lin CY, Seila AC, Flynn RA, McCuine S, Burge CB, Sharp PA, Young RA. 2010. c-Myc regulates transcriptional pause release. Cell 141:432–445. https://doi.org/10.1016/j.cell.2010.03.030.
16. Jang MK, Mochizuki K, Zhou M, Jeong HS, Brady JN, Ozato K. 2005. The bromodomain protein Brd4 is a positive regulatory component of P-TEFb and stimulates RNA polymerase II-dependent transcription. Mol Cell 19:523–534. https://doi.org/10.1016/j.molcel.2005.06.027.
17. Yang Z, Yik JH, Chen R, He N, Jang MK, Ozato K, Zhou Q. 2005. Recruitment of P-TEFb for stimulation of transcriptional elongation by the bromodomain protein Brd4. Mol Cell 19:535–545. https://doi.org/10.1016/j.molcel.2005.06.029.
18. Shilatifard A, Lane WS, Jackson KW, Conaway RC, Conaway JW. 1996. An RNA polymerase II elongation factor encoded by the human ELL gene. Science 271:1873–1876. https://doi.org/10.1126/science.271.5257.1873.
19. Kong SE, Banks CA, Shilatifard A, Conaway JW, Conaway RC. 2005. ELL-associated factors 1 and 2 are positive regulators of RNA polymerase II

elongation factor ELL. Proc Natl Acad Sci U S A 102:10094–10098. https://doi.org/10.1073/pnas.0503017102.
20. Bitoun E, Oliver PL, Davies KE. 2007. The mixed-lineage leukemia fusion partner AF4 stimulates RNA polymerase II transcriptional elongation and mediates coordinated chromatin remodeling. Hum Mol Genet 16:92–106. https://doi.org/10.1093/hmg/ddl444.
21. Simone F, Polak PE, Kaberlein JJ, Luo RT, Levitan DA, Thirman MJ. 2001. EAF1, a novel ELL-associated factor that is delocalized by expression of the MLL-ELL fusion protein. Blood 98:201–209. https://doi.org/10.1182/blood.v98.1.201.
22. Polak PE, Simone F, Kaberlein JJ, Luo RT, Thirman MJ. 2003. ELL and EAF1 are Cajal body components that are disrupted in MLL-ELL leukemia. Mol Biol Cell 14:1517–1528. https://doi.org/10.1091/mbc.e02-07-0394.
23. Simone F, Luo RT, Polak PE, Kaberlein JJ, Thirman MJ. 2003. ELL-associated factor 2 (EAF2), a functional homolog of EAF1 with alternative ELL binding properties. Blood 101:2355–2362. https://doi.org/10.1182/blood-2002-06-1664.
24. Basu S, Barad M, Yadav D, Nandy A, Mukherjee B, Sarkar J, Chakrabarti P, Mukhopadhyay S, Biswas D. 2020. DBC1, p300, HDAC3, and Siah1 coordinately regulate ELL stability and function for expression of its target genes. Proc Natl Acad Sci U S A 117:6509–6520. https://doi.org/10.1073/pnas.1912375117.
25. He N, Chan CK, Sobhian B, Chou S, Xue Y, Liu M, Alber T, Benkirane M, Zhou Q. 2011. Human polymerase-associated factor complex (PAFc) connects the super elongation complex (SEC) to RNA polymerase II on chromatin. Proc Natl Acad Sci U S A 108:E636–E645. https://doi.org/10.1073/pnas.1107107108.
26. Kumari N, Hassan MA, Lu X, Roeder RG, Biswas D. 2019. AFF1 acetylation by p300 temporally inhibits transcription during genotoxic stress response. Proc Natl Acad Sci U S A 116:22140–22151. https://doi.org/10.1073/pnas.1907097116.
27. Takahashi H, Takigawa I, Watanabe M, Anwar D, Shibata M, Tomomori-Sato C, Sato S, Ranjan A, Seidel CW, Tsukiyama T, Mizushima W, Hayashi M, Ohkawa Y, Conaway JW, Conaway RC, Hatakeyama S. 2015. MED26 regulates the transcription of snRNA genes through the recruitment of little elongation complex. Nat Commun 6:5941. https://doi.org/10.1038/ncomms6941.
28. Byun JS, Fufa TD, Wakano C, Fernandez A, Haggerty CM, Sung MH, Gardner K. 2012. ELL facilitates RNA polymerase II pause site entry and release. Nat Commun 3:633. https://doi.org/10.1038/ncomms1652.
29. Rousseaux MW, de Haro M, Lasagna-Reeves CA, De Maio A, Park J, Jafar-Nejad P, Al-Ramahi I, Sharma A, See L, Lu N, Vilanova-Velez L, Klisch TJ, Westbrook TF, Troncoso JC, Botas J, Zoghbi HY. 2016. TRIM28 regulates the nuclear accumulation and toxicity of both alpha-synuclein and tau. Elife 5 https://doi.org/10.7554/eLife.19809.
30. Liu R, Chen C, Li Y, Huang Q, Xue Y. 2020. ELL-associated factors EAF1/2 negatively regulate HIV-1 transcription through inhibition of Super Elongation Complex formation. Biochim Biophys Acta Gene Regul Mech 1863:194508. https://doi.org/10.1016/j.bbagrm.2020.194508.
31. Mourgues S, Gautier V, Lagarou A, Bordier C, Mourcet A, Slingerland J, Kaddoum L, Coin F, Vermeulen W, Gonzales de Peredo A, Monsarrat B, Mari PO, Giglia-Mari G. 2013. ELL, a novel TFIIH partner, is involved in transcription restart after DNA repair. Proc Natl Acad Sci U S A 110:17927–17932. https://doi.org/10.1073/pnas.1305009110.
32. Smith ER, Lin C, Garrett AS, Thornton J, Mohaghegh N, Hu D, Jackson J, Saraf A, Swanson SK, Seidel C, Florens L, Washburn MP, Eissenberg JC, Shilatifard A. 2011. The little elongation complex regulates small nuclear RNA transcription. Mol Cell 44:954–965. https://doi.org/10.1016/j.molcel.2011.12.008.
33. Hu D, Smith ER, Garruss AS, Mohaghegh N, Varberg JM, Lin C, Jackson J, Gao X, Saraf A, Florens L, Washburn MP, Eissenberg JC, Shilatifard A. 2013. The little elongation complex functions at initiation and elongation phases of snRNA gene transcription. Mol Cell 51:493–505. https://doi.org/10.1016/j.molcel.2013.07.003.
34. Harris SL, Levine AJ. 2005. The p53 pathway: positive and negative feedback loops. Oncogene 24:2899–2908. https://doi.org/10.1038/sj.onc.1208615.
35. Luo RT, Lavau C, Du C, Simone F, Polak PE, Kawamata S, Thirman MJ. 2001. The elongation domain of ELL is dispensable but its ELL-associated factor 1 interaction domain is essential for MLL-ELL-induced leukemogenesis. Mol Cell Biol 21:5678–5687. https://doi.org/10.1128/MCB.21.16.5678-5687.2001.